T.C.
DOKUZ EYLUL UNIVERSITY
IZMIR INTERNATIONAL BIOMEDICINE AND GENOME INSTITUTE

GENERATION OF LACRIMAL GLAND FROM INDUCED PLURIPOTENT STEM CELLS

MELİS ASAL

MOLECULAR BIOLOGY AND GENETICS

MASTER OF SCIENCES THESIS

İZMİR-2020

Thesis ID: DEU.IBG.MSc.2017850039

T.C.
DOKUZ EYLUL UNIVERSITY
IZMIR INTERNATIONAL BIOMEDICINE AND GENOME INSTITUTE

GENERATION OF LACRIMAL GLAND FROM INDUCED PLURIPOTENT STEM CELLS

MOLECULAR BIOLOGY AND GENETICS

MASTER OF SCIENCES THESIS

MELİS ASAL

Supervisor: Assoc. Prof. Dr. Sinan Güven

TÜBİTAK 117S264

(This research was supported by TÜBİTAK grand number 117S264 and TÜBA-GEBİP)

THESIS ID : DEU.IBG.MSc.2017850039

Dokuz Eylül Üniversitesi İzmir Uluslararası Biyotıp ve Genom Enstitüsü Genom Bilimleri ve Moleküler Biyoteknoloji Anabilim Dalı, Moleküler Biyoloji ve Genetik Yüksek Lisans programı öğrencisi Melis Asal **'GENERATION OF LACRIMAL GLAND FROM INDUCED PLURIPOTENT STEM CELLS'** konulu Yüksek Lisans tezini 16.06.2020 tarihinde başarılı olarak tamamlamıştır.

Doç. Dr. Sinan Güven

BAŞKAN

ÜYE
Doç. Dr. Canan Aslı Yıldırım
Dokuz Eylül Üniversitesi

ÜYE
Prof. Dr. Gülperi Öktem
Ege Üniversitesi

YEDEK ÜYE
Prof. Dr. Esra Erdal Bağrıyanık
Dokuz Eylül Üniversitesi

YEDEK ÜYE
Doç. Dr. Özden Yalçın Özuysal
İzmir Yüksek Teknoloji Enstitüsü

Dokuz Eylul University Izmir International Biomedicine and Genome Institute Department of Genomics and Molecular Biotechnology, Molecular Biology and Genetics graduate program Master of Science student Melis Asal has successfully completed her Master of Science thesis titled '**GENERATION OF LACRIMAL GLAND FROM INDUCED PLURIPOTENT STEM CELLS'** on the date of 16.06.2020.

Assoc. Prof. Sinan Güven
CHAIR

MEMBER
Assoc. Prof. Canan Aslı Yıldırım
Dokuz Eylül University

MEMBER
Prof. Dr. Gülperi Öktem
Ege University

SUBSTITUTE MEMBER
Prof. Dr. Esra Erdal Bağrıyanık
Dokuz Eylül University

SUBSTITUTE MEMBER
Assoc. Prof. Özden Yalçın Özuysal
İzmir Institute of Technology

TABLE OF CONTENTS

INDEX OF TABLES

INDEX OF FIGURES

LIST OF ABBREVIATIONS

2.5D	2.5-Dimensional
2D	2-Dimensional
3D	3-Dimensional
BF	Bright field
BSA	Bovine Serum Albumin
cDNA	Complementary DNA
CE	Conjunctival Epithelium
DAPI	4',6-Diamidino-2-Phenylindole, Dihydrochloride
DED	Dry Eye Disease
DM	Differentiation Medium
DMEM/F12	Dulbecco's Modified Eagle's Medium and Ham's F-12 Nutrient Mixture
ECM	Extracellular Matrix
EDM	Eye Field Differentiation Medium
ELISA	Enzyme Linked Immunosorbent Assay
FACS	Fluorescence Activated Cell Sorting
FGFR2b	FGF Receptor 2(III)b
FGFs	Fibroblast Growth Factors
FC	Flow Cytometry

GAGs	Glycosaminoglycans
GAPDH	Glyceraldehyde 3-Phosphate Dehydrogenase
hESC	Human Embryonic Stem Cells
hiPSCs	Human Induced Pluripotent Stem Cells
ICC	Immunocytochemistry
IHC	Immunohistochemistry
KSR	Knockout Serum Replacement
MMPs	Matrix Metalloproteinases
MZOC	Multi Zonal Ocular Cells
NC	Neural Crest
Ndst1	N-deacetylase/N-sulfotransferase
OCT	Optimal Cutting Temperature
ODM	Ocular Cell Differentiation Medium
OSE	Ocular Surface Ectoderm
PBS	Phosphate Buffered Saline
PFA	Paraformaldehyde
POM	Periocular mesenchyme
qPCR	Quantitative Polymerase Chain Reaction
RT	Room temperature

SEAM	Self-Formed Ectodermal Autonomous Multi-Zone
Tm	Primer Melting Temperature
UV	Ultraviolet
ΔG	Gibbs Free Energy

ACKNOWLEDGEMENTS

I would first like to thank my thesis advisor Assoc. Prof. Sinan Güven. The door to his office was always open to discuss anything. He always believed in my ideas, and allowed me to make decisions about the project but still led the way whenever I felt lost. He has thought me how to think scientifically, and for that I will always be grateful for him. I would also like to thank to Assoc. Prof. Canan Aslı Yıldırım for her support throughout my thesis. Throughout this Master's study, I was supported by TUBITAK 2210-A scholarship, which I appreciate a lot.

My dear lab collegues Emine Kahraman and Ibrahim Halilullah Erbay, thank you for the companionship and putting up with my stress throughout the three years. I will forever miss having scientific conversations with you. And I will always remember the fun we had. All of the present and previous Güven lab members, especially Gizem Aktuğ, Ali Kemal Baş and Olcay Burçin Akbulud, thank you for sharing ideas with me and sharing expertise. I appreciate them a lot.

Resul Özbilgiç, I would not accomplish this far if it weren't for your help. Whether it was scientific discussing, running to my help whenever I felt like I lost control with the experiments, or supporting me through long hours spent in the lab, you were always wise and patient. I will forever cherish your support. Sezgin Bal and Yusuf Cem Eskiocak, without the two of you, I would totally get lost, and lose even more cells, in the world of flow cytometry. Thank you for taking time and sharing expertise. I also must express my gratitude towards the members of IBG imaging, flow cytometry and histopathology core facility members; especially Melek Üçüncü and Didem Çimtay, for spending long hours with me in the way of gathering beautiful images. I also would like to thank to Soheil Akbari for showing me everything I know about iPSC culture and to Prof.Dr. Esra Erdal for sharing cells with us.

Finally, my biggest thanks to my parents Nazan Asal and Izzet Asal for providing me with unfailing support and continuous encouragement not only for the years of study, but throughout my life. I dedicate this thesis to them, and to my grandparents, who supported me throughout the journey.

GENERATION OF LACRIMAL GLAND FROM INDUCED PLURIPOTENT STEM CELLS

Melis Asal, Izmir International Biomedicine and Genome Institute, Dokuz Eylul University Health Campus, Balcova, 35340, Izmir/Turkey

ABSTRACT

Lacrimal gland secretes tear fluid, which moistens and protects the eye surface. Lacrimal gland deficiency related dry eye disease causes discomfort and can lead to inflammation, infection and even vision loss. The common treatment method is artificial tears however they do not contain the biologically active components of real tear and do not offer a cure. Human induced pluripotent stem cells harbor the potential to differentiate into all three germ layers and thus can be employed to construct a 3-dimensional functional lacrimal gland tissue *in vitro*. During development, interaction between periocular mesenchyme and conjunctival epithelium gives rise to the lacrimal gland.

The aim of this thesis is to differentiate human induced pluripotent stem cells into lacrimal gland tissue. We hypothesize that human induced pluripotent stem cells can give rise to functional lacrimal gland and the tear proteins secreted from this construct can offer an alternative for artificial tears used in dry eye disease.

For this purpose, different approaches have been investigated. The differentiation processes were monitored with cell marker expression in the RNA and protein level. Results demonstrate that extended culture of multi zonal ocular cells spontaneously formed 3-dimensional functional lacrimal gland mimicries. To our knowledge, this is the first functional lacrimal gland construct reported containing both tissue specific epithelial and mesenchymal cells derived from human induced pluripotent stem cells.

Keywords: Lacrimal gland, Human induced pluripotent stem cells, Dry eye disease, Stem cell differentiation.

UYARILMIŞ PLURİPOTENT KÖK HÜCRELER KULLANILARAK LAKRİMAL BEZİN GELİŞTİRİLMESİ

Melis Asal, İzmir Uluslararası Biyotıp ve Genom Enstitüsü, Dokuz Eylül Üniversitesi, Sağlık Kampüsü, Balçova, 35340, İzmir/Türkiye

ÖZET

Lakrimal bez, göz yüzeyini nemlendirip koruyan gözyaşını üretmekle sorumludur. Lakrimal bezin işlevselliğinin bozulmasından kaynaklanan kuru göz; rahatsızlık hissi, iltihap ve hatta görüş kaybına sebebiyet verebilir. Yaygın tedavi yöntemi yapay gözyaşı kullanımıdır. Fakat yapay gözyaşları gerçek gözyaşının biyolojik olarak aktif bileşiklerini içermez ve şifa sağlamaz. İnsan uyarılmış pluripotent kök hücreleri üç germ tabakasına farklılaşma potansiyeline sahiptir ve *in vitro* 3 boyutlu fonksiyonel lakrimal bez geliştirilmesi için kullanılabilir. Gelişim sürecince, perioküler mezenkim ve konjonktiva epiteli arasındaki etkileşim lakrimal bez oluşumunu sağlar.

Bu çalışmanın amacı insan uyarılmış pluripotent kök hücrelerini lakrimal bez dokusuna farklılaştırılmasıdır. Çalışmanın hipotezi, insan uyarılmış pluripotent kök hücrelerinin fonksiyonel lakrimal beze farklılaşabileceği ve bu yapı tarafından üretilen gözyaşı proteinlerinin yapay gözyaşı yerine kuru göz hastalığında bir alternatif olabileceğidir.

Bu amaçla farklı yaklaşımlar araştırılmıştır. Farklılaşma süreçleri, hücre tiplerine özgü belirteçlerin RNA ve protein düzeyinde ifadeleri ile gözlemlenmiştir. Sonuçlar, çok zonlu oküler hücrelerin uzun süreli kültürünün 3 boyutlu fonksiyonel lakrimal bez yapılarına kendiliğinden farklılaştığını göstermiştir. Bildiğimiz kadarıyla, bu, insan uyarılmış pluripotent kök hücrelerinden türetilmiş dokuya özgü hem epitel hem de mezenkimal hücreleri içeren bildirilen ilk fonksiyonel lakrimal bez yapısıdır.

Anahtar Sözcükler: Lakrimal bez, İnsan Uyarılmış Pluripotent Kök Hücreleri, Kuru göz, Kök hücre farklılaşması.

1. INTRODUCTION AND GOALS

1.1. Statement and Importance of the Problem

Dry eye disease (DED) is defined as "a multifactorial disease of the ocular surface that cause irritability, visual disturbances and instability of the tear film and can potentially damage the ocular surface". It is accompanied with increased osmolarity of the tear film and inflammation of the ocular surface. DED is investigated in two categories; aqueous deficient and evaporative (Buckley 2018). Aqueous deficient DED emerges due to lacrimal gland (LG) damage or absence and has serious clinical consequences. The commonly accepted approach for DED therapy is the use of artificial teardrops, anti-inflammatory drugs and punctal occlusion (Buckley 2018; Conrady et al., 2016). However in patients with inflammatory aqueous deficient DED, inflammatory mediators and cell accumulation lead to permanent loss of function and fibrosis in the LG as the disease progresses. In these patients, employed therapies are often not sufficient to prevent LG atrophy (Conrady et al., 2016; Bron et al., 2017).

Among the alternative clinical therapy options, regenerative medicine approaches gain importance (Hirayama et al., 2015; Villatoro et al., 2017). Stem cells are defined as cells that can differentiate into another cell type and can self-renew. Induced pluripotent stem cells (iPSCs) are obtained via reprogramming stromal cells into embryonic stages through introducing reprogramming factor genes. Organoids are miniaturized versions of organs mimicking the tissue micro anatomy and function. Organoids generated through use of stem cell technologies offer new research and therapy options. Evolving stem cell technologies make it possible to develop tissue-specific organoids (Takahashi et al., 2007; Yamanaka 2012; Asal and Güven 2020). When generated using patient derived hiPSCs, organoids offer a source for personalized medicine in terms of drug testing. Disease modelling can also be achieved. In addition to these, hiPSC-derived organoids can potentially replace the function of the diseased tissue/organ.

In this thesis, human iPSCs (hiPSCs) are preferred due to their potential use in tissue regeneration and replacement of function of LGs in DED. In this context, tear produced from hiPSC derived tissue constructs can offer a therapy option for aqueous deficient DED.

1.2. Purpose of the Research

The purpose of this thesis is to differentiate hiPSCs into a LG construct by employing various approaches. To find a proper protocol for differentiation, LG markers and tear secretion are analyzed. Through this, we aim to produce native-like tear that can substitute artificial tears used in the treatment of DED.

1.3. Hypothesis of the Research

In this study, we hypothesize that functional human lacrimal gland mimicries can be obtained by differentiating hiPSCs.

2. GENERAL INFORMATION

2.1. Lacrimal Gland

Lacrimal gland is a tubuloacinar exocrine gland that is responsible for the production of the aqueous layer of the tear film. LG secretes and stores water, proteins, peptides and electrolytes that are released into the conjunctival sac through the puncta. The gland also acts as a part of the secretory immune system by secreting immunoglobulins (Örge and Boente 2014; Garg and Zhang 2017).

Tear film offers a protective layer on cornea and lubricates and moistens both cornea and conjunctiva. Along with lubricating the ocular surface and protecting it, tear film also contributes to smooth surface formation for refraction required for optimum visual performance. The film plays roles in maintaining the ocular surface metabolism and protects the ocular surface (Paulsen and Berry 2006). Tear film consists of three layers; the lipid layer, aqueous layer and mucous layer. Lipid layer, also called the external layer, is found in the outermost layer and is secreted by Meibomian gland. Its function is to avoid tear evaporation. Aqueous layer, the middle layer, is produced by the LG and makes up over 90% of the tear film. Mucous layer, the innermost layer, is produced by the conjunctival goblet cells and acts by fixing the tear film to ocular surface (Örge and Boente 2014; Garg and Zhang 2017) (Figure 1).

Tear secreted from human LG varies in composition according to the type; basal, reflex and psycho-emotional. Basal tear production starts during the fetal life even before LG is fully maturated. Reflex tear secretion starts just after birth and plays a role in protecting the ocular surface in the case of damage, foreign body presence and inflammation (Murube 2009). Reflex tear is rich in proteins required for restoring the homeostasis (Tsubota 1998). Psycho-emotional tearing begins in the months following birth. Psycho-emotional tearing is merely associated with emotions rather (Murube 2009).

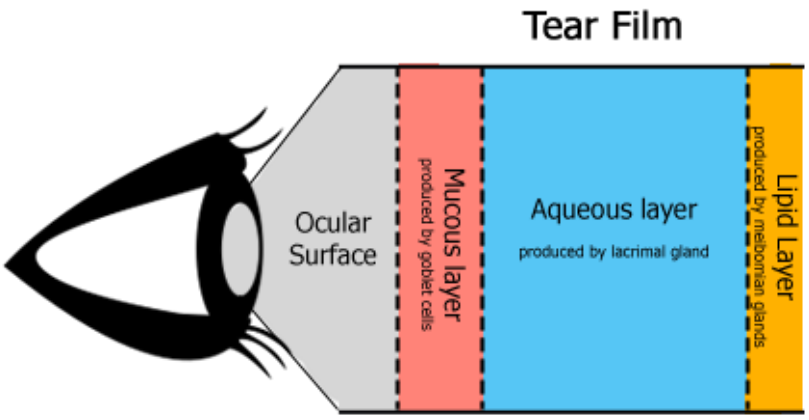

Figure 1 The tear film. Tear film is composed of three layers; mucous, aqueous and lipid layers produced by the conjunctival goblet cells, LG and meiobian gland respectively.

In humans, LG is located at the upper temporal orbit where it is connected to a duct system by which the secretions are delivered to the ocular surface (Figure 2). The gland is divided by the levator aponeurosis into two lobes namely orbital and palbepral. The artery that feeds the LG is the lacrimal branch of the ophthalmic artery. The veins are drained by the superior ophthalmic vein through the same path as the artery. The average size of the LG is 20 mm in length and 12 mm in width and the orbital and palpebral lobes are 5 mm and 3 mm thick respectively. The acini and intralobular ducts of each lobe drain into about 8-12 main excretory ducts, which drain into the superotemporal conjunctival fornix (Conrady et al., 2016).

Stimulation of the LG depends on the ocular surface inputs and also emotional inputs (Bron et al., 2017). The LG is innervated by corneal and conjunctival sensory afferent nerves along with parasympathetic and sympathetic efferent nerves. The nerve terminals are found near the acini, ducts, myoepithelial cells of the LG and also around blood vessels to regulate the quantity and quality of the secretion in response to stimulation of the ocular surface (Bron et al., 2017; Garg and Zhang 2017) (Figure 2). Innervating parasympathetic nerves release acetylcholine, vasoactive intestinal peptide while sympathetic nerves release norepinephrine. These neurotransmitters stimulate secretion and release of proteins, electrolytes and water from the acinar

cells. Other neurotransmitters and neuropeptides released by the innervating nerves are neuropeptide Y, substance P, and calcitonin gene related peptide (Murube 2009).

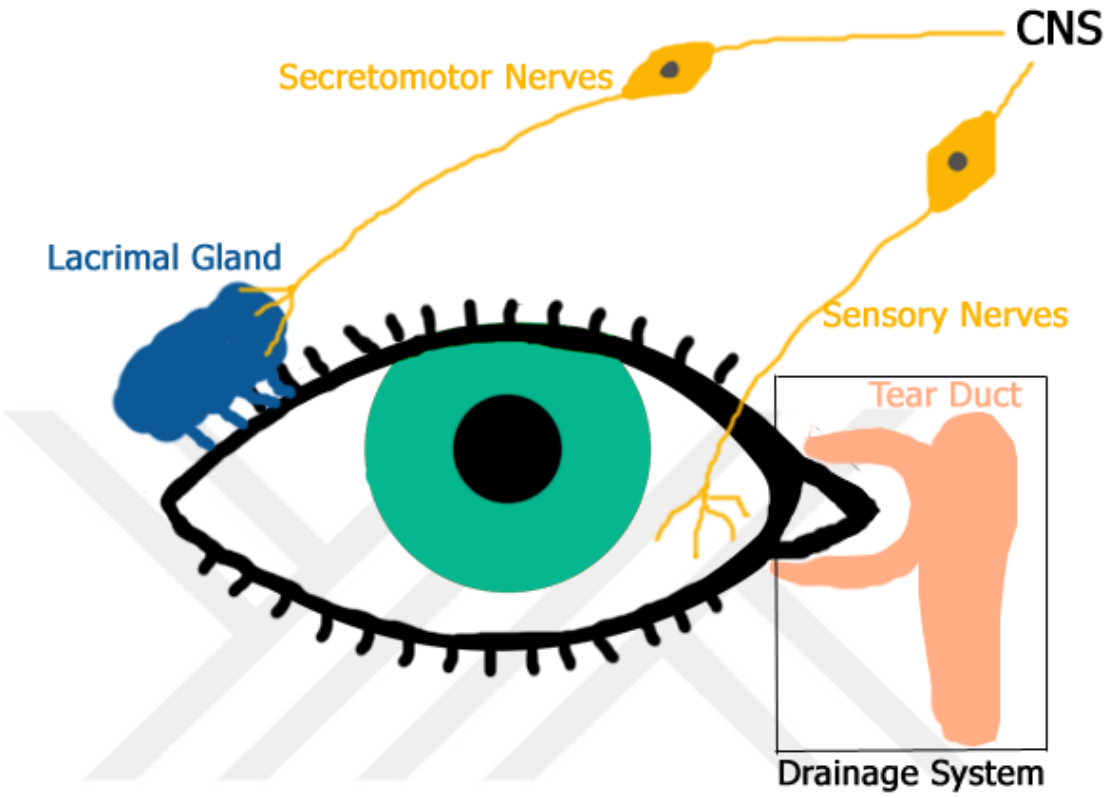

Figure 2 LG functional unit. The unit consists of the LG, secretomotor efferent and sensory afferent nerves and the lacrimal drainage system (Rocha et al., 2008).

2.1.1. Lacrimal Gland Cell Types and Function

The LG epithelia consist of three main cell types; acinar, ductal and myoepithelial.

The secretory units, also called acinus, consist of the secretory cells, the acinar cells. Acinar cells form about 80% of LG cell population. The cells are polarized and possess tight junctions at the lumen which divide their membranes into apical and basolateral parts (Figure 3). Neurotransmitter and neuropeptide receptors are found at the basal part of the cells (Paulsen and Berry 2006). The prominent endoplasmic reticulum and Golgi apparatus, mitochondria of the acinar cells along with the nucleus are located in the basal compartment of the cells. The secretory vesicles are

positioned in the apical side. Acinar cells synthesize, store and unilaterally secrete water, electrolytes, proteins (lysozyme, lactoferrin, growth factors) and mucins (secreted or membrane bound MUC1, MUC4, MUC5B, MUC5AC, MUC6, MUC7 and MUC16) in response to neural and hormonal stimuli (Figure 3). The secreted proteins mainly possess antibacterial properties, the role of mucins on the other hand is not well known except some local roles (Bron et al., 2017). Acinar cells can be stimulated by androgens, estrogens, glucocorticoids, mineralocorticoids, retinoic acid, prolactin, a-melanocyte-stimulating hormone, adrenocorticotropic hormone, luteinizing hormone, follicle-stimulating hormone, growth hormone, thyroid-stimulating hormone, arginine, vasopressin, oxytocin, thyroxine, parathyroid hormone, insulin, glucagons, melatonin, human chorionic gonadotropin, cholecystokinin and somatostatin (Paulsen and Berry 2006).

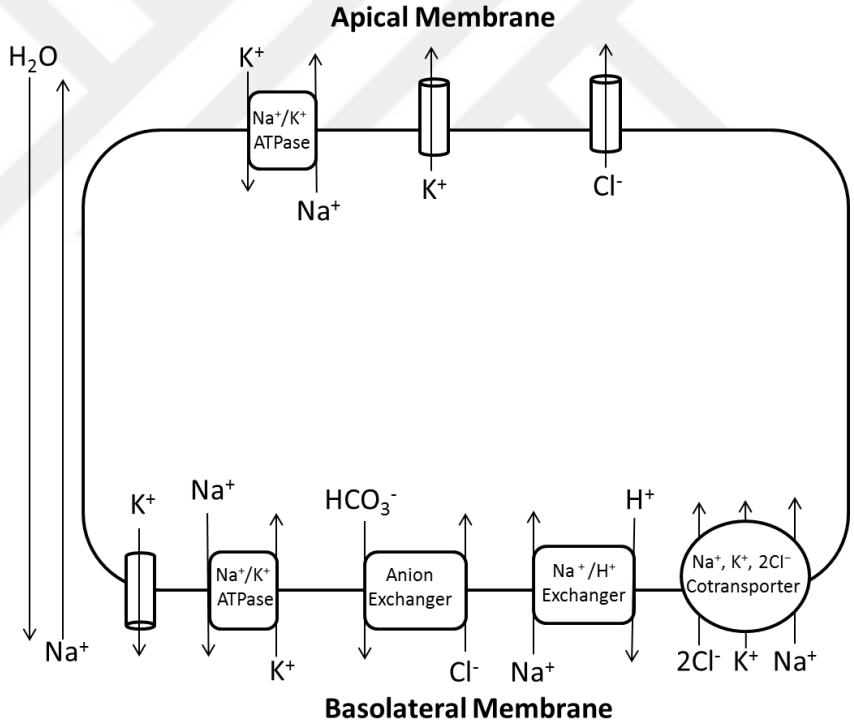

Figure 3 Electrolyte transportation process driving water secretion in LG acini (Selvam et al., 2007).

The acinar cells are attached to the ducts from their apical parts. The secretory ducts are lined by cuboidal cells in one layer in the beginning of ducts and in two layers in the bigger sections of the ducts (Figure 4). These cells comprise about 10–12% of the LG cells and secrete 30% of the LG secretion. The ductal cells modify the secretions of the acinar cells by secreting mainly water and electrolytes. The secretion is mainly a KCl-rich solution, which leads to the K^+ rich LG secretome (Bron et al., 2017). Protein secretion, to a limited extent, also takes place by the basal cells of the ducts. These cells secrete bactericidal permeability-increasing protein, which possesses antibacterial activity in tears. Similar to the acinar cells, the ductal cells are also connected apically by tight junctions, giving rise to polarized cells. The basal sides of the cells on the other hand are linked with gap junctions. The nucleus is located in the basal part of the cells while the endoplasmic reticulum and the Golgi apparatus are found in the apical side (Garg and Zhang 2017; Paulsen and Berry 2006).

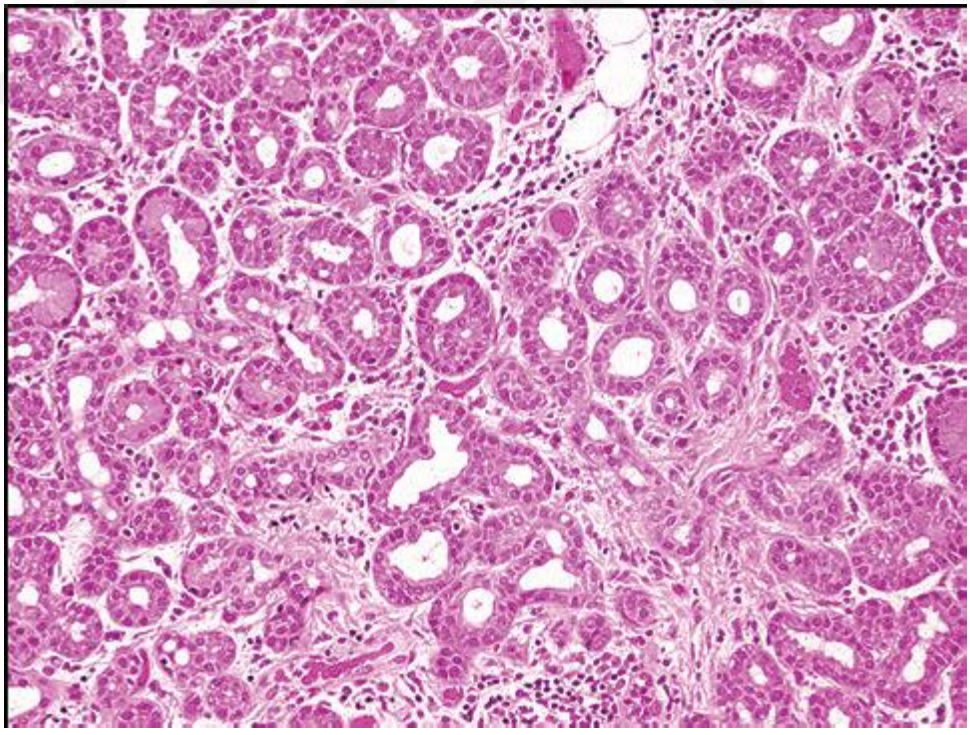

Figure 4 Histology of human LG. This figure was adopted from Conrady et al., 2016.

Myoepithelial cells surround acinar and ductal cells from their basal sides to form a functional network (Bron et al., 2017; Garg and Zhang 2017; Paulsen and Berry 2006). Myoepithelial cells are connected via gap junctions and desmosomes. These cells express muscle proteins (α smooth muscle actin, myosin, tropomyosin) and are thought to exert pressure to acini to expel secretions into the ducts (Bron et al., 2017). They contain receptors for acinar cell stimulating neurotransmitters. Myoepithelial cells are also thought to have a role in preserving the shape of the gland (Garg and Zhang 2017; Paulsen and Berry 2006).

The vascular system also carries immune cells such as plasma cells (IgA, IgG, IgE, IgM, IgD expressing), B and T cells, mast cells (histamine and matrix protein secreting), dendritic cells, macrophages and bone marrow-derived monocytes into the LG, making it a part of the ocular mucosal immune system (Bron et al., 2017; Garg and Zhang 2017; Paulsen and Berry 2006). The immune cells inhabit the interstitial space. Among these cells, IgA expressing plasma cells outweigh the others by number. The secreted IgA is dimeric and is transported along with J spice and secretory component into acinar and ductal cells. T cells are the second most common immune cell type found in the LG. Among T cell types, CD8+ ones predominate in the ducts, interstitium and the space between acini. CD4+ T cells are found mostly in follicles and as aggregates. These cells are found in the interstitial space, in follicles and sometimes among acinar cells. B cells are located in follicles and as aggregates and single cells. In addition to duct lining cells, B cells and dendritic cells express human leukocyte antigen D-related (Bron et al., 2017).

2.1.2. Lacrimal Gland Development

Being an ectodermal gland, epithelial-mesenchymal interaction plays the main role in the development of LG. During LG development, this interaction occurs between conjunctival epithelium (CE) derived from the ocular surface ectoderm (OSE) and periocular mesenchyme (POM) derived from neural crest (NC) (Garg and Zhang 2017). LG development is independent from retina and lens formation (Swindell et al., 2008).

In humans LG development is classified into three stages (Figure 5). In the presumptive glandular stage, CE thickens due to the interaction with the surrounding POM at around 6-7 weeks of gestation. In the epithelial bud stage, CE invades the condensed POM and the ducts are formed around 12 weeks of gestation. Visible lumen formation inside epithelial buds takes place. In the glandular maturity stages, the gland starts taking its mature/adult morphology. The resulting structure is a branched secretory gland. Even though the LG is fully developed during the time of birth, the excretory function is gained about 6 weeks postnatal (Örge and Boente 2014; Garg and Zhang 2017; Dean et al., 2004; Makarenkova et al., 2000).

Figure 5 Human LG development timeline. Thickening of the epithelium occurs around week 6-7 of gestation due to the interaction with the mesenchyme. Elongation of the epithelial bud occurs around 12 weeks. Branching morphogenesis and further maturation occurs after 12 weeks.

Numerous cellular signaling takes place during branching morphogenesis regulate LG development. PAX6 expression in the CE is the first step of LG budding (Makarenkova et al., 2000). LG budding is orchestrated by fibroblast growth factors (FGFs); FGF7 and FGF10. FGF7 is expressed in a diffused manner in the POM. On the other hand, FGF10 is expressed in the POM specifically around the developing epithelial bud throughout development. The specific receptor for FGF10 is FGF receptor 2(III)b (FGFR2b). FGFR2b is expressed in CE, in the region where invasion into POM occurs and the epithelial bud forms (Garg and Zhang 2017).

It was shown that FGFR2b knock down results in disrupted LG development. In addition to this, in mouse embryonic explant eye cultures, LG epithelial budding can be induced by FGF7 and FGF10. FGF10 is considered to be the main player and the epithelial budding inducer during the LG development since FGF10 knockout mice lack the LG epithelial part even though the mesenchymal component is present. Yet in the FGF7 knockout mice LG develops normally (Makarenkova et al., 2000). A single allele of FGF10 is also considered to be insufficient for LG development. Aplasia of the lacrimal and salivary glands occurs due to a heterozygous loss of function mutation. Moreover, lacrimo-auriculo-dentodigital syndrome occurs due to missense mutations in the FGF10 gene (Garg and Zhang 2017).

Proteoglycans within the extracellular matrix (ECM) of the POM regulate the concentration of FGF10 protein. During LG development, glycosaminoglycans (GAGs) attached to proteoglycans limit the diffusion of FGF10 and controls induction of budding. Knockout of UDP-glucose dehydrogenase, the GAG biosynthetic enzyme, was shown to result in excessive FGF10 diffusion and accompanying disrupted epithelial budding (Qu et al., 2012). Matrix metalloproteinases (MMPs) 2 and 9 are secreted by the epithelium to boost the release of FGF10 from the POM ECM (Garg and Zhang 2017). BARX2, along with FGF10, was shown to play a role in LG bud elongation and regulating expression of MMP2 and MMP9 to remodel ECM with a positive feedback mechanism (Tsau et al., 2011).

Heparan sulfates act as co-receptors for the formation of FGF signaling complex assembly. Branching occurs with the growth of the tip of the bud cells. N-deacetylase/N-sulfotransferase (Ndst1) is specifically expressed in the tip cells and not in the stalk, suggesting a role in branching. It was shown that knocking out Ndst1 in the epithelium abolishes the budding by interrupting N-sulfation of heparan sulfates, indicating a role in FGF10 compartmentalization (Pan et al., 2008).

Growth factors among numerous signaling pathways have critical importance in maintenance of histology and function of LG. BMP7 acts mainly on the LG mesenchyme. BMP7 plays parts in mesenchymal condensation and proliferation,

which are both critical for the branching morphogenesis. BMP7, having a complex expression pattern, is initially expressed in the POM around the epithelial bud but later is expressed both by the POM and CE (Dean et al., 2004).

2.1.3. Dry Eye Disease

Dry eye disease affects hundreds of million cases worldwide. It is defined as; a multifactorial disease of the ocular surface that is characterized with loss in tear film homeostasis along with ocular symptoms such as discomfort and visual problems. Neurosensory anomalies such as tear film instability, hyperosmolarity, ocular surface inflammation and damage play roles in DED (Buckley 2018; Rocha et al., 2008). Due to its detrimental effects on quality of life and work efficiency, DED causes economic burdens on individuals and society. Moderate and severe DED leads to prominent pain, restrictions in daily performance, deterioration of quality of life and depression. In severe cases, in addition to deterioration of health quality, DED can lead to ulcer and corneal melting which can result in vision loss (Gayton 2009; Phadatare et al., 2015) (Figure 6).

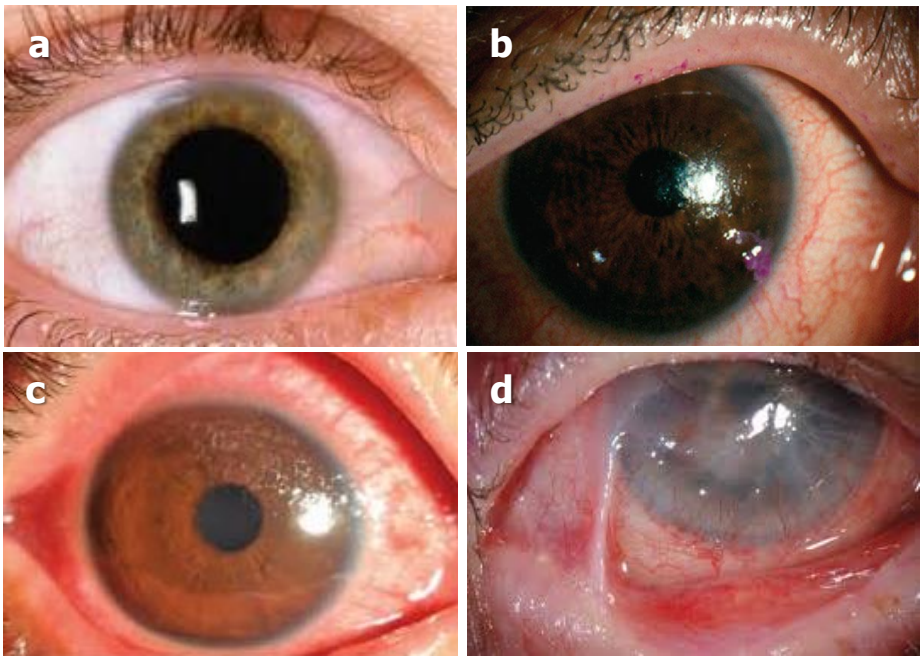

Figure 6 The effect of DED on ocular surface. Cases with a) Severity level 1 b) Severity level 2 c) Severity level 3 d) Severity level 4.

DED is mainly categorized as aqueous deficient dry eye, caused by decreased tear secretion from LG under normal evaporative conditions, and evaporative dry eye, caused by extensive evaporation in the presence of a normal functioning LG (Buckley 2018).

Sjögren syndrome is a chronic and progressive autoimmune disease characterized with systemic complications related to lymphocytic infiltration of exocrine glands, autoantibody production and immunocomplex accumulation (Conrady et al., 2016; Rocha et al., 2008). Inflammation of tear and salivary glands leads to dry eye and dry mouth symptoms. Inflammatory cell infiltration of the LG causes destruction of acini and ducts and aqueous tear loss. In addition to this, inhibition of cytokine, antibody and neurotransmitter secretion or inflammation related secretomotor innervation damage contributes to a decrease in lacrimal secretion (Rocha et al., 2008). Apoptosis is seen in conjunctival epithelium and LG acinar cells (Conrady et al., 2016).

Non-Sjögren dry eye is a type of aqueous deficient type DED without an accompanying autoimmune disorder and can be either congenital or acquired. Causes of Non Sjögren dry eye can be sarcoid granuloma of LG, infiltration of LG with lymphoma and neurofibroma, human immunodeficiency virus infection of LG, Steve Johnson syndrome, mucous membrane pemphigoid, graft-versus-host disease related inflammation, vitamin A deficiency, facial nerve palsy, LG ablation, trauma and radiotherapy (Conrady et al., 2016; Bron et al., 2017).

Primary LG deficiency can be caused by various disorders. Congenital alacrima is an inherited disorder observed during childhood or in young ages. It can be associated with blepharophimosis, LADD, Pierre-Robin syndrome and Allgrove syndrome (Bron et al., 2017; Garg and Zhang 2017). Familial dysautonomia (Riley Day Syndrome) is an autosomal recessively inherited disorder with abnormal development of sensory innervation of the ocular surface and sympathetic and parasympathetic innervation of the LG (Conrady et al., 2016; Bron et al., 2017). In addition to insufficient tear secretion from the LG, due to decrease in sensory

innervation, reflex tearing also decreases. Triple A Syndrome (Allgrove Syndrome) is an autosomal recessively inherited disorder with the congenital loss of LG (Bron et al., 2017). Age related DED is the most common form of DED. Along with the age, tear secretion decreases due to loss of LG secretory tissues, decrease in sensory transmission from the ocular surface and reduced secretory neurotransmitters. Lifelong exposure to oxidative stress leads to tissue damage in LG, decrease in tear volume and increase in osmolarity. Along with advancing age, decrease in the amount of LG related proteins lactoferrin, lysozyme and peroxidase was detected. After the age of 40 the increase in T cell infiltration in the LG leads to destruction in acini and ducts (Conrady et al., 2016; Rocha et al., 2008).

Secondary LG deficiency can be due to LG infiltration, obstruction of LG ducts and reflex hyposecretion. LG infiltration can be caused by sarcoidosis, lymphoma, viral infections, graft-versus-host disease and LG damage secondary to radiation (Conrady et al., 2016; Phadatare et al., 2015)(Conrady et al., 2016; Phadatare et al., 2015)(Conrady et al., 2016; Phadatare et al., 2015) (Conrady et al., 2016; Phadatare et al., 2015). Due to the infiltration, LG cannot function properly; tear secretion decreases and aqueous deficient type DED emerges (Phadatare et al., 2015). Obstruction of LG ducts is related to graft-versus-host disease, Steven Johnson Syndrome, mucous membrane pemphigoid, Trachoma, thermal and chemical burns. With the obstruction of the LG and accessory gland ducts with fibrosis the aqueous layer is affected. Due to goblet cell damage resulting from fibrosis and inflammation, mucin layer, and due to obstruction of Meibomian gland ducts, the lipid layer gets affected. Obstruction can result in opacification of the cornea, perforation and blindness. Tear secretion is regulated by the nervous system. Disruption in the nerves in this pathway can lead to reflex hyposecretion (Conrady et al., 2016; Bron et al., 2017).

2.1.3.1. Treatment Options

The common goal is to restore homeostasis on the ocular surface, overcome inflammation and to maintain long-term ocular surface comfort. Various treatment acting on numerous mechanisms options exist and each one has their advantages and disadvantages. While artificial tear drops are the most commonly used agent against aqueous deficient DED, biological agents, punctal occlusion, stimulation of tear secretion, anti-inflammatory agents, mechanical dacryo-reservoir, salivary gland transplantation are also employed as treatment options (Buckley 2018; Conrady et al., 2016; Gayton 2009; Phadatare et al., 2015) (Table 1).

Artificial teardrops are not aimed at the underlying physiopathology, and are mainly palliative for the replacement of the tear film. With the use of artificial teardrops, the ocular surface is moisturized, tear osmolarity is decreased and the inflammatory agents are diluted. Tear is a complex structure containing water, electrolytes, proteins, lipids and growth factors. Artificial teardrops fail to mimic this complexity. What is more, in contrast to the continuous secretion of tear to the ocular surface, artificial tear drops are used sporadically and the ocular surface cannot be kept moist long term. To increase the thickness of the tear film, duration on the ocular surface and goblet cell density, viscosity-increasing agents are used (Buckley 2018; Conrady et al., 2016). However with the increase in viscosity, blurred vision and deposit formation on eyelids and eyelashes may occur. Single use preparations do not contain preservatives but are more costly. On the other hand, containing preservatives restricts the use of multi dose artificial teardrops. Long term exposure to preservatives causes toxic changes on the ocular surface (Phadatare et al., 2015). Some substances have been developed to decrease the toxicity risk related to chronic exposure to preservatives. pH balancing buffers are used for the stabilization of the activity of artificial tear drops. However these agents have also caused adverse effects such as calcifications in the cornea and epithelial toxicity in long term intensive use (Gayton 2009).

Table 1 Existing treatment options for aqueous deficient DED.

Artificial Tear Drops	Mimics the tear film with the lubricant agent formulations (Buckley 2018)
Biological Agents	• Autologous serum (Villatoro et al., 2017) • Adult allogeneic serum (Villatoro et al., 2017) • Umbilical cord serum (Villatoro et al., 2017)
Punctal Occlusion	A punctum or both puncta are blocked temporarily or permanently (Phadatare et al., 2015)
Tear Secretion Stimulation	• Diquafosol (Byun et al., 2016) • Rebamipide (Kinoshita et al., 2014) • Pilocarpine (Senba et al., 2011) • Cevimeline (Ono et al., 2004)

Anti-Inflammatory Agents	• Topical corticosteroids (Yang et al., 2006)
	• Cyclosporin A (Gao et al., 2013)
	• Tacrolimus (Moscovici et al., 2012)
	• Non-steroid anti-inflammatory agents
	  ○ Diclofenac (Sawazaki et al., 2014)
	  ○ Ketorolac (Sandoval et al., 2007; Weber et al., 2012)
	  ○ Indomethacin (Weber et al., 2012)
	• Lubricin (Schmidt et al., 2013)
	• Topical Interleukin 1 Receptor Antagonist (Amparo et al., 2013)
	• Anti TNF-α (Choi et al., 2016)

Mechanical Dacryo-Reservoir	An artificial tear reservoir is placed subcutaneously in the abdominal wall and is connected to the eye through a catheter (Murube et al., 2003)
Salivary Gland Transplantation	Autologous transplantation of salivary glands to conjunctival fornix in order to replace LG (Wakamatsu et al., 2017)

Autologous serum is rich in albumin, fibronectin and growth factors, and is biochemically similar to human tear (Buckley 2018; Villatoro et al., 2017). It is used in severe ocular surface diseases like Steven Johnson syndrome, Sjögren syndrome and chemical burns. Autologous serum was shown to decrease proinflammatory cytokine release, increase number of goblet cells, increase mucin expression in conjunctiva and accelerate corneal healing. Allogeneic serum is an option for old or infant patients and patients with chronic anemia and systemic infections. There is a risk of immune response but the use of ABO matched donors decreases the risk. Use of serum is restricted due to risk of transmission of blood borne diseases like HIV and hepatitis, decreasing growth factor concentration when stored at 4°C and high cost in long term use. Umbilical cord serum is more advantageous than autologous serum since it can be obtained from more than one donor in high volumes (up to 250 ml) and can be used in multiple patients. Amount of some growth factors in the umbilical cord are higher than in peripheral blood. Ocular surface improvement was achieved in topical use in patients with dry eye resistant to conventional treatment and in patients with graft-versus-host disease (Villatoro et al., 2017).

With punctal occlusion, it is aimed to plug one or both puncta temporarily or permanently to block tear drainage and preserve the existing tear on the ocular surface (Phadatare et al., 2015). It is mainly used in aqueous deficient DED patients. Occlusion is usually carried out with plugs but surgical options also exist. The most common complication of this application is spontaneous plug extrusion. Besides that, infection, migration of the plug to canaliculi pyogenic granuloma, punctal expansion and tumor formation can be observed (Conrady et al., 2016).

2.2. Induced Pluripotent Stem Cells

Stem cells possess ability of unlimited self-renewal and also differentiation. Under proper stimulation stem cells can both differentiate into the desired cell type by dividing symmetrically, and copy itself and form a differentiated cell by dividing asymmetrically (Asal and Güven 2020; Sekhar and Bisht 2006).

Interaction of stem cells with other stem cells or differentiated cells around them along with presence of adhesion molecules, ECM components, growth factors, cytokines and other environmental conditions (pH, metabolites etc.) have effects on proliferation and differentiation of stem cells (He et al., 2009).

Stem cells are categorized according to their differentiation potentials. Cells that are present from the presence of zygote up until the blastocyst stage are totipotent and have the ability to form the embryo and extraembryonic structures such as placenta and amniotic membrane. In the blastocyst stage the inner cell mass are pluripotent and form the organs and tissues by differentiating into all three germ layers; ectoderm, mesoderm and endoderm. Adult stem cells, which can differentiate into a single germ layer are called multipotent. Adult stem cells are found rarely in tissues and organs and have repair roles in the cases of cell death and tissue damage. Cells that can self-renew and can differentiate into one or two cell lines are called oligopotent and cells that can only self-renew are called unipotent stem cells (Mitalipov and Wolf 2009).

The discovery of embryonic stem cells and directed differentiation of these cells into desired cell lines to grow functional tissue and organs have led to the thought of transplanting them into patients as a cure. Although embryonic stem cells harbor great potential as cell sources for regenerative medicine, the isolation method hinders their use in human applications. Embyronic stem cell isolation requires destruction of the embryo and is therefore considered unethical.

iPSCs were first generated in 2006 by reprogramming mouse fibroblasts into embryonic stem cell-like cells through introduction of OCT4, SOX2, C-MYC and KLF4 genes (Takahashi and Yamanaka 2006). In 2007, the same transcription factors were used to reprogram human fibroblasts into hiPSCs (Takahashi et al., 2007). These cells resemble embryonic stem cells and retain the ability to differentiate into cells of all three germ layers.

Due to high pluripotent cell efficiency, skin fibroblast cells are mainly preferred for reprogramming. Alternative choices have also been investigated due to burdens

associated with these cells; the need for skin biopsy, risk of infection, probable mutation due to ultraviolet (UV) exposure and 3-4 week time to obtain the cells. Easy-to-obtain peripheral blood cells have become another source. It was shown that nuclear cells; granulocytes, monocytes, B and T lymphocytes and progenitor cells can be reprogrammed to gain pluripotent potency (Karagiannis et al., 2018).

Numerous methods are employed for reprogramming. During reprogramming with retroviruses and lentiviruses, the genes to be introduced are added into the viral genome. After the virus infects a cell, it integrates its genome into the cell genome and due to the integrated transcription factors, the cell gains character. The risk of integration of the viral genome into an active gene of the cell and causing a mutation is the biggest disadvantage of this method. As non-integrating methods, Adeno virus and Sendai virus are used (Yamanaka 2012). Non-viral transfection methods have also arisen. IPSCs were obtained with transfecting the cells with plasmids. As non-viral reprogramming methods, episomal, piggy-BAC transposon, synthetic mRNA, recombinant proteins and small molecules were studied and iPSCs were obtained (Yamanaka 2012; Karagiannis et al., 2018).

For the reprogramming, cells (fibroblasts, peripheral blood cells etc.) are obtained from either healthy or diseased individuals. The cells are reprogrammed with the introduction of defined transcription factors and iPSCs develop. The cultured cells are examined for their pluripotent character. When examined morphologically, the cells resemble embryonic stem cells with their round morphology with big nuclei and tight cytoplasm and by adhering strongly to the plate and forming dense colonies with sharp borders. iPSCs have been shown to express pluripotency markers OCT3/4, NANOG, SOX2, SSEA4 and TRA-1-60. To verify the pluripotency of the cells, cells that have been shown to express these markers are tested for their differentiation potentials *in vitro* and *in vivo*. In *in vitro* cell culture iPSCs form embryonic bodies. In *in vivo* differentiation test, the iPSCs are injected into mice with severe combined immunodeficiency to assess for teratoma (Marti et al., 2013). Formation of embryonic bodies and teratoma confirm the pluripotency character of the cells.

Even though allogeneic transplantation is an available treatment option for some diseases, scarce in donors and immune rejection limits their use. By mimicking the organogenesis during embryonic stages, through distinct protocols, hiPSCs can be differentiated into many cell types. This phenomenon harbors great hope for tissue/organ regeneration or transplantation. Being able to obtain patient specific hiPSCs overcomes ethical issues and the risk of immunological response. Since patient derived hiPSCs possess the same human leucocyte antigens with the patient, it overcomes the problem of rejection. Moreover, through *in vitro* genetic disease models, a better understanding of pathogenesis is achieved. iPSCs derived tissues/organs also take place in drug and toxicology studies. The main goal of regenerative medicine applications is to use hiPSCs to obtain transplantable cells/tissues/organs artificially.

Human iPSCs have been employed to obtain various tissues. Human iPSC derived mature cardiomyocytes, vocal fold epithelial mucosa, retinal pigment epithelial cells, kidney organoids and functional hepatic organoids are some of the many examples (Ronaldson-Bouchard et al., 2018; Lungova et al., 2019; Low et al., 2019; Akbari et al., 2019; Mandai et al., 2017).

2.3. Tissue Engineering and Regenerative Medicine Approaches for Lacrimal Gland

Tissue engineering and regenerative medicine field employs interdisciplinary approaches to construct functional mimicries/biological substitutes to recapitulate tissues/organs for various purposes (Khademhosseini and Langer 2016). These substitutes can be used for personalized medicine and drug testing purposes and can potentially replace or regenerate tissues/organs. Cells, tissue scaffolds and cell stimulating factors are major components of tissue engineering. In tissue engineering, cells are isolated from healthy or diseased tissue and primary adult/stem/progenitor cells are identified. The term regenerative medicine is usually applied when the case especially involves the use of progenitor/stem cells. These cells are then expanded *in vitro* on a scaffold. Conditions required for organogenesis

are provided; bioactive molecules such as tissue specific growth factors and cytokines are added to obtain a functional tissue (Berthiaume et al., 2011).

As long-term treatment options for DED, LG regenerative studies have utmost importance. With the use of tissue engineering principles, it is aimed to construct a functional LG and to transplant it to replace the diseased gland. Cell source, choice of the scaffold, compatibility and sustainability of the cell and scaffold and integration of the construct with sensory/motor neurons must be taken into account while trying to regenerate this complex gland. With the help of various methods, 2-dimensional (2D) and 3-dimensional (3D) LG like structures and bioengineered structures have been developed.

In order to obtain an engineered functional LG *in vitro*, investigating the culture conditions of LG cells is essential. Mouse LG epithelial cells have been cultured by numerous groups. Epithelial and mesenchymal LG cells isolated from newborn mice were cultured on basement membrane matrix. Acinar-like epithelial clusters containing secretory granules and AQP-5 expression was observed (Ueda et al., 2009). In another study, LG epithelial cells were isolated from newborn mice and were selectively cultured with cholera toxin. These cells were shown to develop spheres from single cells (Kobayashi et al., 2012).

Functional human LG cultures were also performed *in vitro*. LGs were isolated from exenteration patients. Stem cells and differentiated cells were observed. The LG epithelial cells formed duct-like connections containing "spherules". Lysozyme, sclgA and lactoferrin secretion after carbachol stimulation was observed with ELISA (Tiwari et al., 2012).

Decellularization of the LG is also important as a scaffold option for tissue engineering applications. In 2015, rabbit LG was decellularized and adult rabbit LG progenitor cells were seeded onto the decellularized matrix. The structure was shown to contain 3D acinar and duct-like structures with secretory function (Lin et al., 2015). In another LG study, amniotic membrane was employed as a scaffold to culture rabbit LG cells. Acini-like structures and secretory material accumulation were

observed. Carbachol stimulation resulted in β-hexosaminidase secretion (Schrader et al., 2007).

The organ germ method is based on the recapitulation of the damaged tissue or organ's developmental processes during the organogenesis. With this method, ectodermal organs such as teeth and hair follicles were developed and studies were conducted to develop ectodermal secretory organs such as the salivary gland and LG *in vitro*. To assess the usability of this method for LG regeneration, epithelial and mesenchymal cells were isolated from E16.5 mice LG. The cells showed branching morphogenesis, bud elongation and invagination mimicking the organogenesis. When this bioengineered LG was transplanted into aqueous deficient mice, formation of connection between the bioengineered LG and the host duct to drain tears to the ocular surface was observed. The bioengineered LG contained acini, duct, myoepithelial cells, nerve fibers and showed functionality. The ocular surface problems associated with the aqueous deficiency were fixed with the transplantation of the bioengineered LG (Hirayama et al., 2015; Hirayama et al., 2013).

iPSCs are a promising potential source for LG bioengineering. Human embryonic stem cells, similar to iPSCs in nature were assessed for their differentiation potential into LG epithelial cells in a study conducted in 2017. Microarray analysis of mice embryonic or adult LG and related organs was conducted to identify transcription factors involved in LG epithelial organogenesis. These transcription factors were transfected via synthetic messenger RNAs into human embryonic stem cells. Overexpression of PAX6, SIX1 and FOXC1 led to formation of LG epithelial-like cells with increased expression of epithelial markers, branching morphogenesis markers and LG markers (Hirayama et al., 2017).

3. MATERIALS AND METHODS

3.1. Type of Research

This study is an *in vitro* experimental study.

3.2. Date and Location of Research

Whole research was conducted between 2017 September – 2020 March in Izmir Biomedicine and Genome Center (IBG).

3.3. Universe and Sample of Research

In this thesis scope, primary human samples were not used.

3.4. Materials of Research

hIPSCs reprogrammed in the laboratory of Assoc. Prof. Tamer Önder (Koç University, Istanbul, Turkey) were obtained from Prof. Dr. Ş. Esra Erdal Bağrıyanık (IBG Center, Izmir Turkey) on 01.03.2019.

3.5. Variables of the Research

Independent variables: Matrigel® concentration, differentiation medium components, duration of differentiation culture

Dependent variables: Marker expression in the RNA and protein level, heterogeneity of the differentiated cells, ability to be subcultured, cell morphology

3.6. Data Collection Methods

3.6.1. Human Induced Pluripotent Stem Cells Culture

WT1 hiPSCs generated as explained in Akbari et al., 2019 were used in this thesis (Akbari et al., 2019). The cells were kept in their pluripotent state by changing the medium daily and passaging every 7 days. The cells that morphologically seemed differentiated were scraped from the surface with the help of a sterile pipette tip.

mTeSR1 (STEMCELL Technologies) medium was used to culture hiPSCs. The medium was prepared by mixing the mTeSR1 supplement with mTeSR basal medium in a 1:4 (v/v) ratio. The mixture was supplemented with 1% (v/v) Penicillin-Streptomycin (Pen-Strep, Gibco, Thermo Fisher Scientific). The cells were maintained on Matrigel® (Corning) at all times. Matrigel® was stored at -20°C and was thawed on ice at 4°C refrigerator. When thawed, Matrigel® was kept on ice at all times to avoid gelation.

Matrigel® coating was carried out by mixing 10-14 µl (depending on the gelation factor of each lot) of Matrigel® with 1ml of serum free Dulbecco's Modified Eagle's Medium and Ham's F-12 Nutrient Mixture (DMEM/F12) (Gibco, Thermo Fisher Scientific) medium on ice. This mixture was sufficient to coat a single well of a 6-well plate. Once the mixture was transferred to the wells, the plate was placed in a 37°C 5% CO_2 cell culture incubator for 1h. After 1h, the plate was used for cell seeding, or was stored either at 4°C refrigerator or in an incubator for up to a week.

Adherent hiPSCs were passaged every 7 days. To passage hiPSCs, the medium was aspirated and the well was washed with 1 ml of serum free DMEM/F12. 1 ml of ReLeSR (STEMCELL Technologies) was added to the well and was incubated at room temperature (RT) for 1 min. After 1 min, ReLeSR was aspirated and the now empty well was transferred to the 37°C incubator for 4 min. 1 ml of mTeSR1 containing 10 µM ROCK inhibitor (Y-27632; Tocris Bioscience) was transferred to the pre-Matrigel®-coated well. After the incubation period, a 2 ml serological pipette was used to detach the cells from the surface by flushing with 1 ml of mTeSR1. The detached colonies were collected with the serological pipette while trying not to render the colonies to single cells. A drop of the cell solution was added to the Matrigel® coated mTeSR1 containing well and was cultured at 37°C with 5% CO_2 in an incubator.

3.6.2. Human Induced Pluripotent Stem Cells Differentiation

Two different approaches were employed for *in vitro* LG generation from hiPSCs. The first approach consists of two branches. In one branch, the hiPSCs were differentiated into POM cells while on the other branch the cells were differentiated into Self-Formed Ectodermal Autonomous Multi-Zone (SEAM) to obtain CE cells (Figure 7). The main goal was to combine these two differentiated cell types in a 3D matrix to support LG formation.

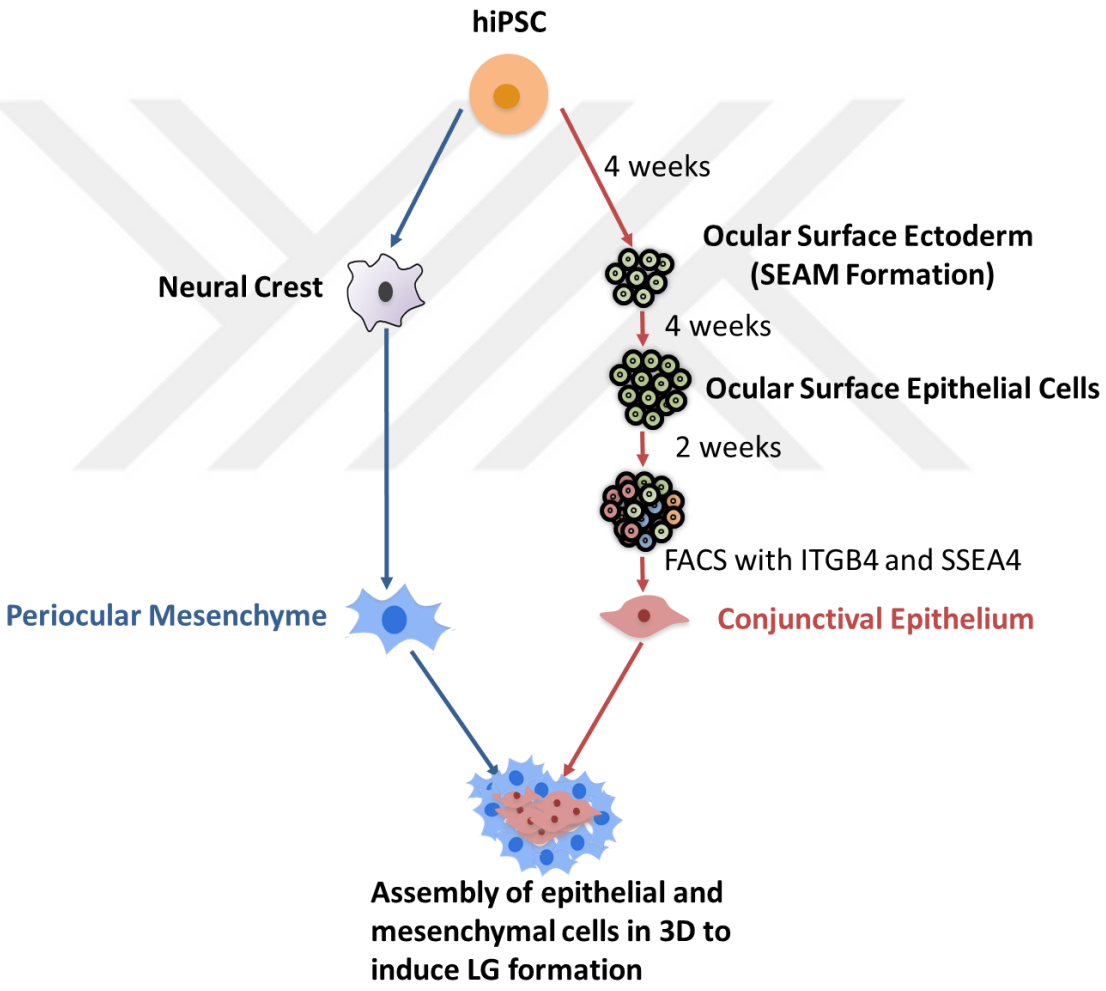

Figure 7 The first approach, including separately differentiating hiPSCs into POM and CE cells and further combining them in a 3D matrix to allow cell interaction and LG formation.

The second approach employs Multi Zonal Ocular Cell (MZOC) generation and aims to differentiate CE and POM cells simultaneously in the same culture system and allow spontaneous development of a LG mimicry (Figure 8).

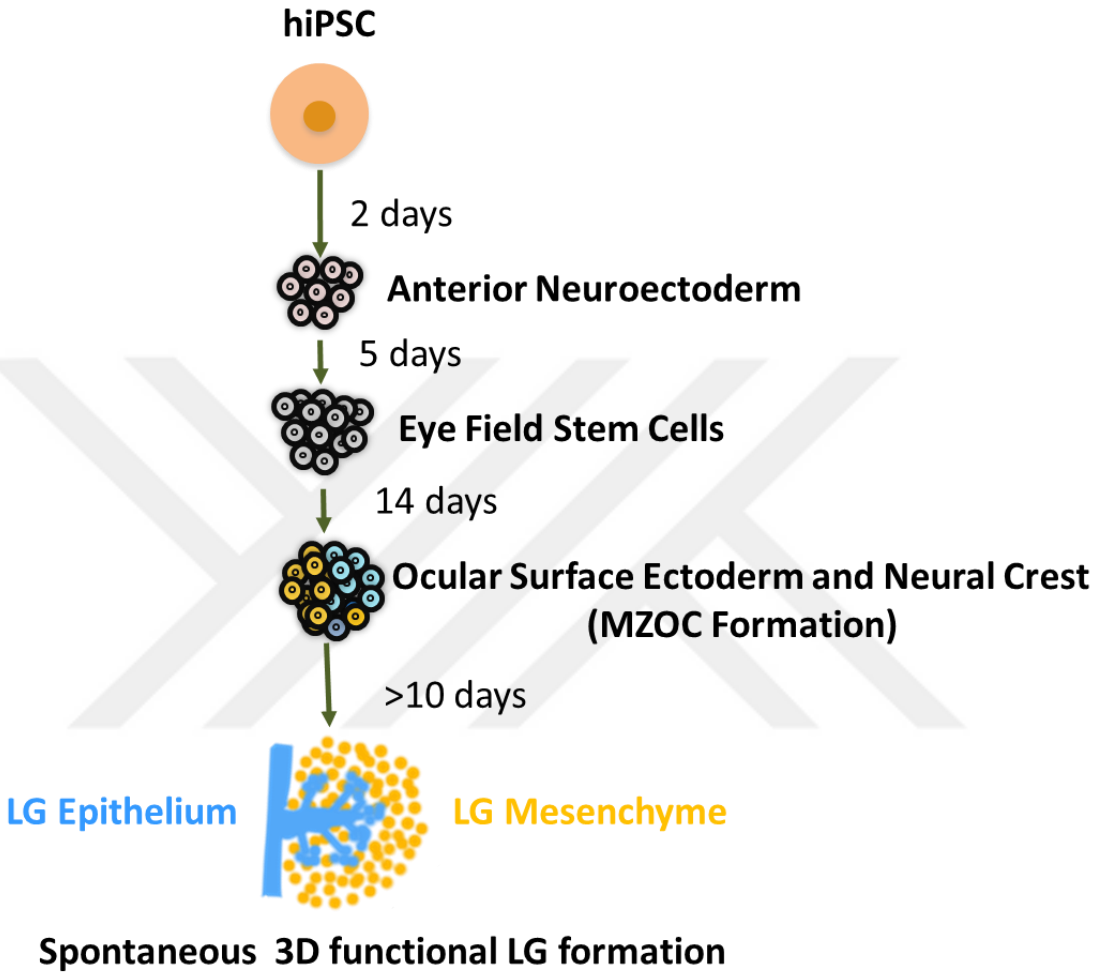

Figure 8 The second approach, involving simultaneous differentiation of hiPSCs into LG progenitor cells and further maturation into a spontaneously formed functional LG construct.

3.6.2.1. Periocular Mesenchyme Differentiation

POM cells were differentiated from hiPSCs by adapting the work published by Lovatt and colleagues about differentiating human embryonic stem cells into POM cells (Lovatt et al., 2018).

HiPSCs maintained in mTeSR for one week were dissociated into single cells with Accutase (Gibco, Thermo Fisher Scientific). In order to do that, media was aspirated and the cells were washed with phosphate buffered saline (PBS; Gibco, Thermo Fisher Scientific) once. Accutase was added and the plate was incubated for 10-15 min in a 37°C incubator. When the cells fully detached, they were collected in fresh mTeSR. The solution was filtered using a 40 µm cell strainer to remove debris and cell clumps. The cells were washed and centrifuged for 5 min at 160xg at RT in mTeSR to remove any remaining Accutase solution. The cells were resuspended in mTeSR containing 10 µM ROCK inhibitorand plated with a density of $1.8x10^4$–$2.5x10^4$ cells/cm^2 on 1% Matrigel® coated plates. 24 h later media was aspirated and fresh mTesR1 supplemented with ROCK inhibitor was added. For following media changes, addition of ROCK inhibitor was omitted. Differentiation was initiated 2 days after seeding (Figure 9).

For induction of differentiation, media was changed to KOSR medium (Knockout DMEM (Gibco, Thermo Fisher Scientific) containing 15% Knockout serum replacement (KSR; Gibco, Thermo Fisher Scientific)) with 10 µM TGF-β inhibitor SB431542 (STEMCELL Technologies). 2 days later media was refreshed. On day 7, media was adjusted by the addition of N2 medium (DMEM/F12 containing 1% 1X N2 MAX supplement (R&D Systems) and 1% Pen/Strep) to make a 75% KOSR medium, 25% N2 medium mix with 10 µM SB431542. On day 9, the media was adjusted to 50% KOSR medium, 50% N2 medium and 10 µM SB431542 and 10 µM Wnt inhibitor IWP2 (STEMCELL Technologies) were added. 8 days after induction of differentiation (day 11), the media was adjusted to 25% KOSR medium, 75% N2 medium with 10 µM SB431542. Finally on day 13, the media was fully converted to N2 medium with 10 µM SB431542 and 10 µM IWP2 (Figure 9).

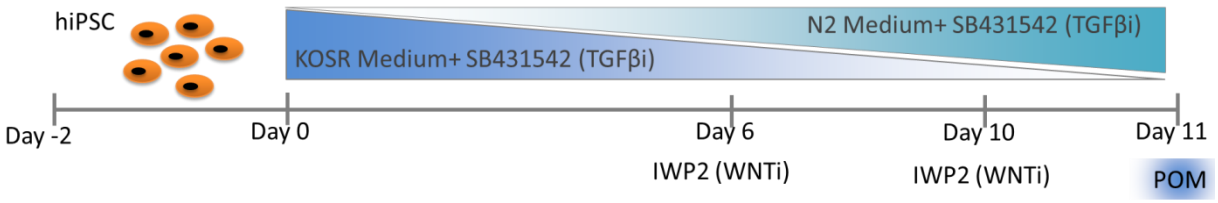

Figure 9 POM differentiation protocol timeline.

In some instances, the POM were further maintained after the differentiation, in these cases the cells were cultured in N2 medium with 10 µM SB431542.

3.6.2.2. Self-Formed Ectodermal Autonomous Multi-Zone Differentiation

HiPSCs were differentiated into eye field cells by adapting the protocol published by Hayashi and colleagues in 2016 and 2017 (Hayashi et al., 2016; Hayashi et al., 2017).

For hiPSC culture on Laminin 511 fragments, 9.6 µl of iMatrix-511 (Diagnocine) (4.8 µg) was mixed with 1.99 ml PBS. This 2 ml mixture was used to coat one well of a 6 well plate. The plate was incubated at 37°C for 1h or for 3h at room temperature, or overnight at 4°C. After the incubation, 0.7 ml of StemFit medium (Ajinomoto) was added to the culture plates and the mixed solution was removed. 1.5 ml of StemFit medium (40 ml Medium A and 10 ml Medium B) containing 10 µM Y-27632 was added. The plate was incubated at 37°C in 5% CO_2 for 15 min.

To passage the confluent cells to the StemFit/LN511E8 culture system, media was aspirated and cells were washed once with 1 ml of PBS. 300 µl of dissociation solution (5 ml TrypLE Select (Gibco, Thermo Fisher Scientific) and 5 ml 0.5 mM EDTA (Sigma-Aldrich) was added and the plate was incubated for 5 min at 37°C in 5% CO_2. After the incubation, the dissociation solution was aspirated and the cells were washed with 2 ml of PBS. 1 ml of StemFit medium with 10 µM Y-27632 was added. The cells were detached with the help of a cell scraper. The cells were rendered to single cells by pipetting up and down multiple times. The cells were counted and were seeded on a well of a LN511E8-coated 6 well plate with a density of $1.3x10^4$ cells/well and 1.5 ml StemFit medium with 10 µM Y-27632. Medium was refreshed

the next day without Y-27632 and the cells were incubated for 7 days in total by changing the medium every 2 days. The cells were passaged 3-4 times in the StemFit/LN511E8 culture system before induction of differentiation.

For differentiation, hiPSCs were dissociated with TrypLE Select and were seeded on a LN511E8 coated 6 well plate with a density of 1.500–4.500 cells/well in 1.5 ml StemFit medium with 10 µM Y-27632. Medium was refreshed the next day without Y-27632. The plate was incubated at 37°C in 5% CO_2 for 10 days with changing the medium every 2 days and every day after day 7.

After 10 days of culture in StemFit medium, the media is changed to 2 ml Differentiation Medium (DM: GMEM (Gibco, Thermo Fischer Scientific), 10 ml KSR, 1 mM sodium pyruvate (PAN-Biotech), 0.1 mM nonessential amino acids (NEAA) (Lonza), 500 µl 2 mM l-glutamine (Gibco, Thermo Fischer Scientific), 50 µl Pen/Strep, and 55 µM monothioglycerol (FUJIFILM Wako Pure Chemical Corporation). The plate was incubated at 37°C in 5% CO_2 for 28 days by refreshing the medium every 2 days. At this phase the cells are supposed to form SEAMs.

3.6.2.3. Multi Zonal Ocular Cells Differentiation

HiPSCs were differentiated into eye field cells by adapting the protocol established by Li and colleagues in 2019 (Li et al., 2019).

HiPSCs cultured for 1 week were detached from the surface using ReLeSR while taking care not to disrupt colonies. Colonies were collected with ice-cold eye field differentiation medium (EDM: 24.2 ml DMEM/F12, 24.2 ml neuralbasal medium (Gibco, Thermo Fisher Scientific), 500ul L-GlutaMAX (Gibco, Thermo Fisher Scientific), 500ul NEAA, 100 µl Monothioglycerol (FUJIFILM Wako Pure Chemical Corporation), and 500 µl 1% N2 (R&D Systems)) mixed with 2% Matrigel®. The colonies were seeded on 1% Matrigel® coated wells and placed in a 37°C 5% CO_2 incubator. The next day medium was changed with fresh EDM containing 2% Matrigel®, making the colony culture 2.5D. The colonies were cultured 5 more days in EDM without Matrigel®. After 5 days, the medium was changed to ocular cell

differentiation medium (ODM: 43,9 ml DMEM/F12, 5 ml KSR (Gibco, Thermo Fisher Scientific), 500 µl L-GlutaMAX, 500 µl NEAA, 100 µl Monothioglycerol) and culture was continued up to 120 days in some instances. Media was changed daily (Figure 10).

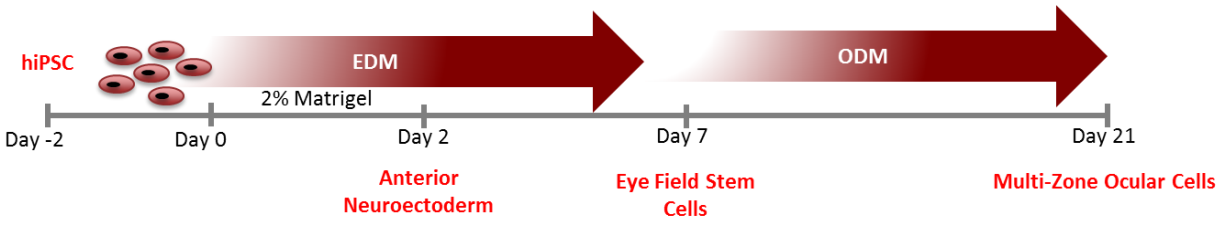

Figure 10 MZOC differentiation protocol timeline.

3.6.3. Cell Characterization

The differentiated cells were analyzed according to their gene and protein expressions. The used methods were Quantitative Polymerase Chain Reaction (qPCR), Immunocytochemistry (ICC), Immunohistochemistry (IHC), Flow Cytometry and ELISA.

Sample preparation for qPCR required RNA isolation, complementary DNA (cDNA) synthesis and primer design.

3.6.3.1. RNA Isolation

TRIzol reagent (Invitrogen) and RNA isolation kit (Macherey-Nagel) were used in RNA isolation. Media was aspirated and the cells were washed with PBS once. TRIzol was added according to the cell number (1 ml TRIzol per 10^6 cells). Cells were scraped and collected. Cell lysate was kept in -80°C until further isolation steps.

The lysate was thawed then homogenized with tissue grinder (ISOLAB) and with pipetting. The lysate was then incubated for 5 min at RT. Chloroform as much as 20% of the TRIzol volume was added. The tube was shaken up and down 20 times and was incubated at RT for 2-3 min. The tube was centrifuged at 12.000xg for 15 min at 4°C to separate the phases. 3 phases formed after separation,

denoting the organic phase containing proteins and lipids, interphase containing DNA and the aqueous phase containing RNA. The aqueous phase was collected and 70% ethanol as much as the volume of collected aqueous phase was added. The sample was mixed by pipetting and was incubated for 10 min at RT.

Isolation proceeded with the NucleoSpin RNA Isolation Kit. The lysate was mixed by pipetting and was transferred into the NucleoSpin RNA column. The column was centrifuged for 30 min at 11.000xg. The column was placed in a new collection tube and 350 µl of membrane desalting buffer was added. The column was centrifuged at 11.000xg for 1 min. DNase reaction mixture was prepared by mixing 10 µl of rDNase with 90 µl of reaction buffer. 95 µl of the DNase Reaction Mixture was added on the center of the column and the column was incubated for 15 min at RT for the reaction to occur. After the incubation, 200 µl of buffer RAW2 was added to the column and was centrifuged at 11.000xg for 30 s. The column was placed into a new collection tube and the column was washed 2 times with 600 µl of buffer RA3 and 250 µl buffer RA3. After the second wash, the tube was centrifuged for 2 min at 11.000xg. The column was placed in a RNase/DNase free eppendorf and RNA was eluted with 40 µl Nuclease free H_2O by centrifuging at 11.000xg for 1 min.

RNA quantity was measured using NanoDrop. A260/280 ratio was aimed to be about 2 and A260/230 ratio required to be above 2 to accept the isolated RNA as being pure. The isolated RNA is kept at -80°C until cDNA synthesis.

3.6.3.2. cDNA Synthesis

ABM OneScript Plus cDNA Synthesis Kit was used for cDNA synthesis and manufacturer's protocol was followed.

RNA templates and the reagents are thawed on ice. A reaction mixture containing RNA, 1 µl of Random Primers (10 µM), 1 µl of dNTP mix (10 mM) and Nuclease Free H_2O up to 14.5 µl was prepared. The mixture was kept at 65°C for 5 min and incubated on ice for 1 min. After the incubation, 4 µl of 5X Reverse Transcriptase Buffer, 0.5 µl RNaseOFF Ribonuclease Inhibitor (40U/µl) and 1 µl

OneScript Plus RTase (200 U/µl) were added. The mixture was incubated at 25°C for 10 min, 50°C for 15 min and the reaction was stopped by heating at 85°C for 5 min. The synthesized cDNA was kept at -20°C until downstream applications.

3.6.3.3. Primer Design

Primers used for differentiation monitoring were chosen according to the genes that are considered markers on literature for each stage of differentiation. Glyceraldehyde 3-phosphate dehydrogenase (GAPDH) was chosen as the housekeeping gene.

Several criteria were taken into account for primer design. In general, a length of 18-25 nucleotides for primers was considered acceptable. Primer Melting Temperature (Tm), the temperature at which half of the DNA duplex will dissociate to become single stranded is another important criterion. Tm of primers were adjusted to be between 59°C and 65°C, and within 5°C of each other at most. GC content should be aimed to be between 50 and 60%, with the 3' of a primer ending in C or G to promote binding. Generally primers with similar GC content were chosen. Primers with at least 2 G or C bases (GC clamp) in the last 5 bases at the 3′ end were also preferred since G-C base pairs form a stronger bonds than A-T base pairs. Runs of 4 or more of the same base, or dinucleotide repeats were avoided when possible, to avoid mispriming.

Presence of the secondary structures can lead to poor yield; adversely affect primer template annealing and thus the amplification. Hairpins occur when two regions of the same primer, complementary in nucleotide sequence when read in opposite directions, base-pair and form an unpaired loop. Hairpins were avoided during the primer design. A primer self-dimer is formed by r interactions between two primers, where the primer is homologous to itself. Primer heterodimers are formed by interactions between the two different primers, where they are homologous. The Gibbs Free Energy (ΔG) is the measure of the amount of work that can be extracted from a process operating at a constant pressure. The stability of a dimer is commonly represented by its ΔG value, the energy required to break the

dimer. Larger negative value for ΔG indicates stable, undesirable dimers. In this thesis, ΔG value bigger than -6 were considered acceptable.

Whenever possible, primer pairs were separated with an intron to eliminate genomic DNA amplification during qPCR. Minimum intron length was adjusted to be 200 and maximum length was chosen as 1000 base pairs.

NCBI Primer Blast was used to design and verify the primers. The designed sequences were synthesized by Oligomer Biyoteknoloji, Ankara. All primers were adjusted to 100 μM by diluting with nuclease-free H_2O and stored at -20°C. Sequences of the primers are depicted in Table 2.

Table 2 Primer Sequences.

Gene	Forward Sequence (5′ -3′)	Reverse Sequence(5′ -3′)
GAPDH	ACCACAGTCCATGCCATCAC	TCCACCACCCTGTTGCTG TA
PAX6	CAGAGCCCCATATTCGAGCC	CAAAGACACCACCGAGCTGA
K13	ACGCCAAGATGATTGGTTTC	CGACCAGAGGCATTAGAGGT
P63	GCAGTCGAGCACCGCCAAGT	TCAAAGCAGCGTCGGCCCAG
PITX2	AGG CCA CTT TCC AGA GGA AC	CGC TCC CTC TTT CTC CAT TT
FOXC1	CATTTTGGTCTAGGGTGGTTTC	TCTGATTGGCAGGGCAGAT
LMX1b	GTGTGAACGGCAGCTACGC	TCATCCTCGCTCTTCACGG
LYZ	GCTGGAGACAGAAGCACTGAT	ATGCCTTGTGGATCACGGAC
AQP5	GAACCCAGCCCGCTCTTTTG	AGTCCTCGTCAGGCTCATACG
K15	ATCGCTACTTACCGCAGCC	CACCTGTCCATCCACTGACTC
K19	ACTACACGACCATCCAGGAC	GAGCCTGTTCCGTCTCAAAC
P75	CAGGACAAGCAGAACACCGT	GGTGTGGACCGTGTAATCCA
M5AC	CGACCTGTGCTGTGTACCAT	GTGCAGGGTCACATTCCTCA
FGF10	GAAATCGGAGTTGTTGCCGTC	TGCCACATACATTTGCCTCC
K13	CAGTGAGATGGAGTGCCAGA	GCTGAGGAAGGGAAACCAATCA

3.6.3.4. Quantitative Polymerase Chain Reaction

For each condition, 3 biological conditions each harboring 3 technical controls were used. GoTaq Master Mix (Promega) was used for qPCR according to the manufacturer's manual. For each cDNA; 5 µl Master Mix, 2 µl H_2O, 1 µl cDNA, 1 µl forward primer (10 ng/µl) and 1 µl reverse primer (10 ng/µl) were mixed in a well of a white 96 well plate. The plate was sealed with a transparent film and centrifuged at 1500 rpm for 2 min. Protocol shown in Table 3 was set up in Roche Lightcycler 480.

Table 3 qPCR Protocol.

Program	**Cycle**	**Temperature (°C)**	**Time (s)**
Pre-incubation	1	95	120
PCR	40	95	10
		60	10
		72	30
Melting	1	95	10
		65	30
Cooling	1	40	30

ΔΔCT values were calculated with Excel (Microsoft, USA). Average of CT_{GAPDH} values was calculated. ΔCT values were calculated as CT_{sample} - CT_{GAPDH}. Averages of $\Delta CT_{control}$ values were taken. To calculate ΔΔCT values, the formula $\Delta CT_{control}$ – ΔCT_{sample} was used and $2^{-\Delta\Delta CT}$ value gave the fold change.

3.6.3.5. Immunocytochemistry Assay

Immunocytochemistry (ICC) was used along other methods to analyze protein expression of the cells. To prepare cells for ICC, the media was aspirated and the cells were washed with PBS 3 times. 4% Paraformaldehyde (PFA; sigma) was added and the cells were incubated at RT for 20-30 min. After incubation, PFA was aspirated and the cells were washed with PBS 3 times. The fixated sample was kept in 4°C refrigerator until blocking/permeabilization.

The staining buffer was prepared as 1% Bovine Serum Albumin (BSA; Sigma-Aldrich) (w/v) and 0.3% Triton-X100 (neoFroxx) (v/v) in PBS. PBS was withdrawn from the samples and staining buffer with the enough volume to cover surface was added. The sample was either incubated for at RT for 2-3 h or at 4°C for overnight. After incubation, primary antibody diluted in the staining buffer was added (Table 4). Sample containing the primary antibody was incubated for overnight at 4°C. After the incubation period the sample was washed with PBS 3 times and secondary antibody diluted in staining buffer was added. The sample was incubated for 3h at RT. After the incubation period the sample was washed 3 times with PBS. 0.5 µg/ml 4',6-Diamidino-2-Phenylindole, Dihydrochloride (DAPI; neoFroxx) was added and the sample was incubated at RT for 20 min. The sample was washed with PBS 3 times and the stained sample was visualized using Fluorescence Microscopy (Olympus IX71).

Table 4 Antibody dilutions for ICC.

Target	Product number	Host	Conjugation	Dilution
OCT3/4	R&D, MAB1759	Rat	Unconjugated	1:50
NANOG	Thermo Fisher, PA5-18406	Goat	Unconjugated	1:100
SOX2	Bioss, bs-5685R	Rabbit	Unconjugated	1:100
PITX2	Novus, NBP2-57409	Rabbit	Unconjugated	1:25
FOXC1	Novus, NB100-1268	Goat	Unconjugated	1:50
PAX6	Novus, NBP2-44576	Mouse	Unconjugated	1:200
TP63	R&D, AF1916	Goat	Unconjugated	1:20
P75	Bioss, bs-0161R	Rabbit	Unconjugated	1:100
K13	Novus, NBP2-38166	Rabbit	Unconjugated	1:50
K12	Santa Cruz, sc-515882	Mouse	Unconjugated	1:250
Anti-rat	Jackson Immuno,712-545-150	Donkey	AF488	1:500
Anti-goat	Jackson Immuno, 705-545-003	Donkey	AF488	1:500
Anti-goat	Jackson Immuno, 705-605-003	Donkey	AF647	1:500
Anti-rabbit	Jackson Immuno, 711-585-152	Donkey	AF594	1:500
Anti-rabbit	Jackson Immuno, 711-545-152	Donkey	AF488	1:500
Anti-mouse	Jackson Immuno, 715-585-150	Donkey	AF594	1:500

3.6.3.6. Immunohistochemistry Assay

IHC was used along other methods to analyze protein expression.

To prepare cells for IHC, the media was aspirated and the tissue was washed with PBS 3 times. 4% PFA was added and the tissue was incubated at RT for 20-30 min. After incubation, PFA was aspirated and the tissue was washed with PBS 3 times. The fixated sample was placed in a 30% sucrose solution and was incubated at 4°C until the tissue sank to the bottom of the tube.

After sinking, the tissue was taken out of the sucrose solution and was placed in Optimal Cutting Temperature (OCT; Fisher Healthcare). Sample was kept in OCT at 80°C until cryosectioning. 5 µm thick sections were cut by the IBG histopathology core facility. The sections were kept at -20°C until staining.

For staining, the slides were thawed at RT for 15 min. The slides were washed with PBS 3 times. The tissues on slides were surrounded by Pap pen (Patolab). Staining buffer was added and the slides were incubated for 1h at RT. After incubation, primary antibody diluted in the staining buffer was added and the slides were incubated at 4°C overnight (Table 5). The slides were washed with PBS 3 times and secondary antibody diluted in staining buffer was added. The slides were incubated at RT for 1 h. The slides were washed with PBS 3 times and DAPI (0.5 µg/ml) was added. After incubation at RT for 10 min, the slides were washed with PBS 3 times. The slides were mounted with mounting medium (Cell Signaling Technology) and were covered with coverslips. The coverslips were sealed with nail polish and the dried slides were kept at dark at 4°C. The slides were visualized with confocal microscopy (Zeiss LSM880).

Table 5 Antibody dilutions for IHC.

Target	Product number	Host	Conjugation	Dilution
PITX2	Novus, NBP2-57409	Rabbit	Unconjugated	1:25
FOXC1	Novus, NB100-1268	Goat	Unconjugated	1:50
PAX6	Novus, NBP2-44576	Mouse	Unconjugated	1:200
TP63	R&D, AF1916	Goat	Unconjugated	1:20
P75	Bioss, bs-0161R	Rabbit	Unconjugated	1:200
K13	Novus, NBP2-38166	Rabbit	Unconjugated	1:1000
K12	Santa Cruz, sc-515882	Mouse	Unconjugated	1:250
AQP5	Bioss, bs-1554R	Rabbit	Unconjugated	1:200
E-cadherin	Bioss, bs-10009R	Rabbit	Unconjugated	1:200
Calponin	Bioss, bs-0095R	Rabbit	Unconjugated	1:100
K15	Novus, NBP1-85602	Rabbit	Unconjugated	1:300
Na^+/K^+ ATPase	Millipore, 05-369-25ug	Mouse	Unconjugated	1:20
N-cadherin	Cell Signaling, 13116T	Rabbit	Unconjugated	1:250
EpCAM	Biolegend, 324203	Mouse	FITC	1:100
Anti-rat	Jackson Immuno, 712-545-150	Donkey	AF488	1:500
Anti-goat	Jackson Immuno, 705-545-003	Donkey	AF488	1:500
Anti-goat	Jackson Immuno, 705-605-003	Donkey	AF647	1:500
Anti-rabbit	Jackson Immuno, 711-585-152	Donkey	AF594	1:500
Anti-rabbit	Jackson Immuno, 711-545-152	Donkey	AF488	1:500
Anti-mouse	Jackson Immuno, 715-585-150	Donkey	AF594	1:500

3.6.3.7. Flow Cytometry

The differentiated hiPSCs were washed once with PBS. 2 ml of Accutase was added and the tissue was incubated for 30 min at 37°C. The still attached tissue parts were scraped. Pipetting was performed several times to dissociate the cells. 150 U/ml collagenase II (Sigma-Aldrich) was added and the tissues were incubated for 45 min at 37°C. The dissociated cells were collected and resuspended in ice-cold medium. The cells were filtered using a cell strainer (40 µm) and the cells were counted. The tube was centrifuged 400xg for 10 min at RT. $1x10^3$ cells/well in 100 µl FACS buffer (0.25% Sodium Azide (Sigma-Aldrich) and 1% BSA were dissolved in 1X PBS) was distributed into wells of a v-bottom 96 well plate. Antibodies were added according to the dilutions listed on Table 6. The plate was incubated at dark on ice for 30 min. The plate was centrifuged at 400xg for 5 min. The wells were washed 3 times. 1 µl DAPI (0.5 µg/ml) per 100 µl was added and the plate was incubated on ice for 15 min. The wells were washed once with PBS and 2 times with FACS buffer. The analyses were carried out using BD Fortessa and FlowJo software.

Table 6 Antibody dilutions for FC.

Target	**Product number**	**Conjugation**	**Dilution**
SSEA4	Biolegend, 330407	AF647	1:50
ITGB	Biolegend, 327807	PE	1:50

3.6.3.8. Fluorescence Activated Cell Sorting

The differentiated hiPSCs were washed once with PBS. 2 ml of Accutase was added and the tissue was incubated for 30 min at 37°C. The still attached tissue parts were scraped. Pipetting was performed several times to dissociate the cells. 150 U/ml collagenase II was added and the tissues were incubated for 45 min at 37°C. The dissociated cells were collected and resuspended in ice-cold medium. The cells were filtered using a cell strainer (40 µm) and the cells were counted. The tube was centrifuged 400xg for 10 min at RT. $1.0x10^3$ cells/well in 100 µl FACS buffer was distributed into wells of a v-bottom 96 well plate. Antibodies were added according

to the dilutions listed on Table 6. The plate was incubated at dark on ice for 30 min. The plate was centrifuged at 400xg for 5 min. The wells were washed 3 times. 1 µl DAPI (0.5 µg/ml) per 100 µl was added and the plate was incubated on ice for 15 min. The plate was washed with PBS once and with FACS buffer 2 times. Sorting was carried out with BD Aria and analysis was done using the FlowJo software.

3.6.3.9. Enzyme Linked Immunosorbent Assay

Lactoferrin secretion detection was carried out with Human Lactoferrin ELISA Kit (Abcam, ab200015) according to the manufacturer's protocol. Fresh standard dilutions were prepared from the provided stock standard for each experiment according to the kit's calculations. Samples were used directly, without any dilution. 2 wells were used as the zero control.

Conditioned cell culture media was collected upon 10 µM forskolin (Tocris Bioscience) induction during different time intervals. The media was centrifuged at 2.000xg for 10 min to remove debris. Sample was kept at -20°C until ELISA experiment.

All samples and reagents were equilibrated to RT before use. 50 µL of either standards or samples were distributed to wells. 50 µL of the Antibody Cocktail was added and the sealed plate was incubated for 1h at RT with continuous shaking at 400 rpm. After the incubation, the wells were washed with 350 µL 1X Wash Buffer PT 3 times. 100 µL of TMB Development Solution was added to the wells and the plate was incubated for 8 min in the dark with continuous shaking at 400 rpm. After the incubation, 100 µL of Stop Solution was added. The plate was shaken for another 1 min for the solution to mix. After the incubation, OD was recorded at 450 nm

3.7. Research Plan

Research Plan	September 2017-September 2018	October 2018-March 2019	March 2019-March 2020	April 2020-May 2020
Literature Review	X	X	X	X
Experiment Planning		X	X	
Data Collection and Experimenting			X	
Evaluation of Data			X	X
Thesis Writing			X	X

3.8. Evaluation of Data

Within the scope of this thesis study, GraphPad Prism 7 program was used to analyze the qPCR findings. ICC and IHC images were analyzed through ImageJ and Zen 3.1 (Blue edition) programs. FC analysis was carried out using FlowJo V10 program.

3.9. Limitation of Research

Common limitation of hiPSC related studies is the variations observed in hiPSCs obtained from different sources. In our study, the hiPSCs showed different response to some protocols from the hiPSCs stated in the literature.

The first approach consisted of purifying the culture system with the use of FACS. However emergence of the COVID-19 pandemic hindered the research and the research facility closed, disabling conductance of further studies.

3.10. Ethics Committee Approval

This thesis was approved by the Non-Invasive Research Ethical Committee of IBG with the protocol number 2020-019 on 16.05.2020. The thesis approval is presented in Section 8.1.

4. RESULTS

4.1. Pluripotency Marker Expression of hiPSCs

hiPSC colonies maintained the pluripotent colony morphology with sharp edges and with round cells with big nuclei and tight cytoplasm (Figure 11 a and b). Expression of pluripotency markers, NANOG, OCT3/4 and SOX2 transcription factors were detected with ICC localized to the nuclei of cells (Figure 11 c and d), indicating that cells maintained their pluripotent character during the expansion culture.

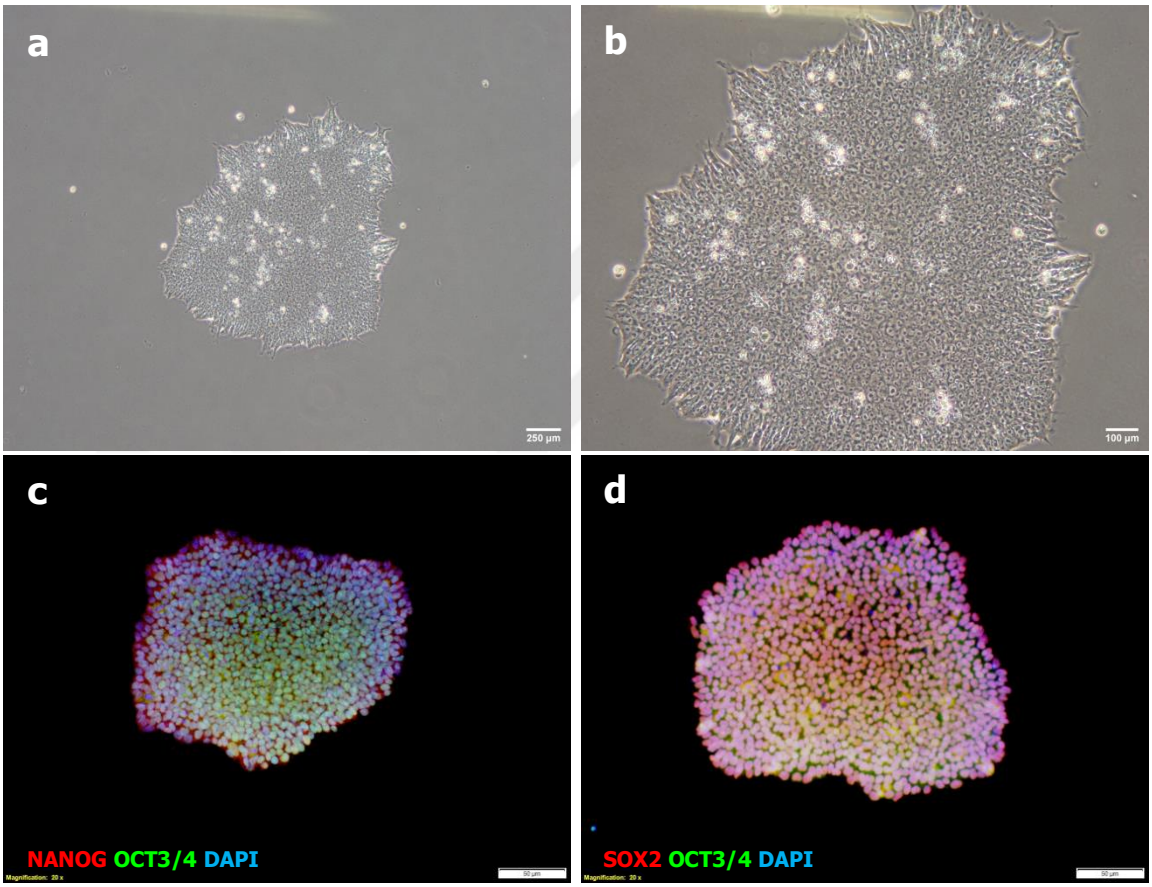

Figure 11 hiPSC culture a) Bright field (BF) picture of hiPSCs with pluripotent characteristic morphology during culture, b) BF picture of hiPSCs with pluripotent characteristic morphology during culture in a closer view c) hiPSC colony stained against pluripotency markers NANOG and OCT3/4, d) hiPSC colony stained against pluripotency markers SOX2 and OCT3/4. Nuclei are stained with DAPI.

4.2. Formation of POM

HiPSCs seeded as single cells with $1.8x10^4$–$2.5x10^4$ cells/cm^2 density on 1% Matrigel® coated plates were maintained in mTesR1. The cells maintained their pluripotent morphology until induction of differentiation (Figure 12 a). After 2 days, differentiation was initiated. Following one week of differentiation, distinct changes in cell morphology was observed as the culture system became heterogeneous with formations resembling "islands" (Figure 12 b). As the differentiation proceeded, the culture became confluent, with cells forming adherent clumps (Figure 12 c). At the end of the differentiation process, the culture system was highly heterogeneous and confluent (Figure 12 d).

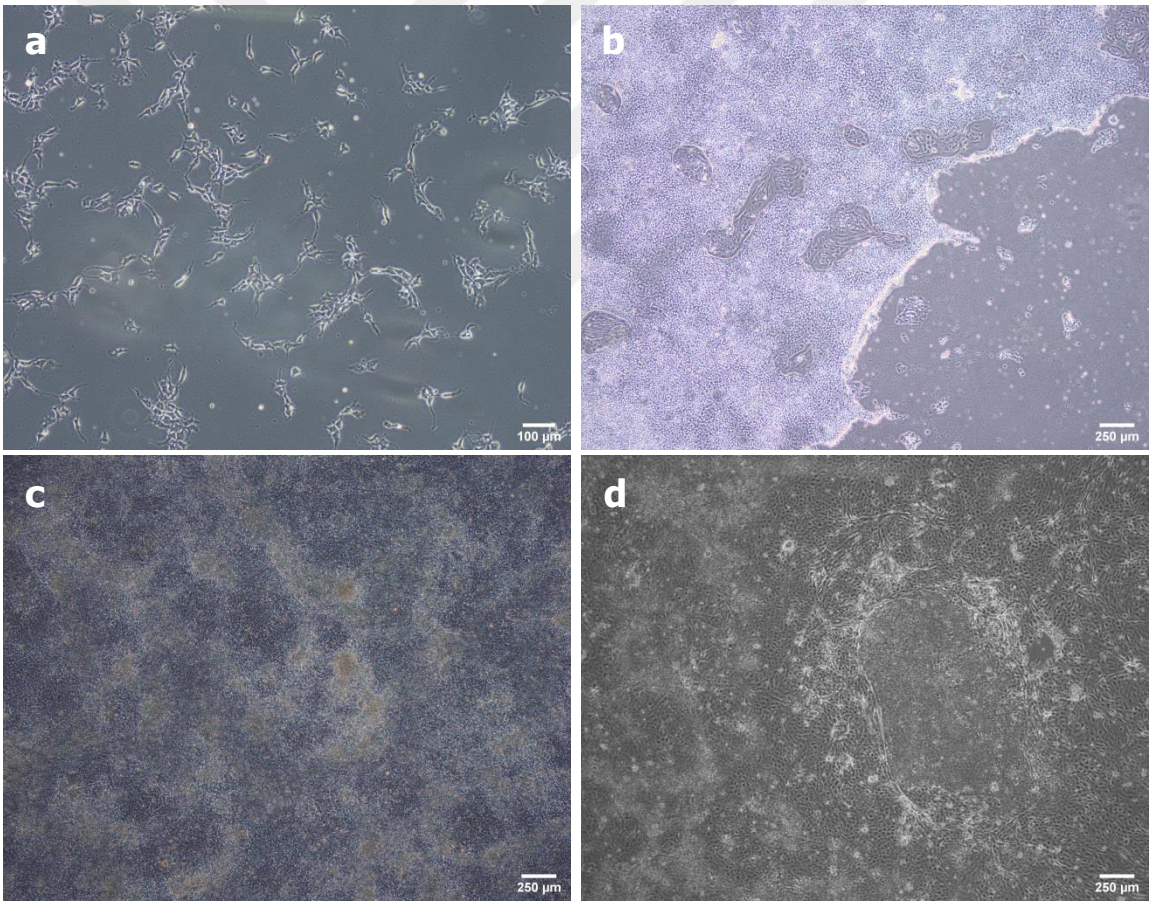

Figure 12 BF images of POM differentiation on a) Day 1, b) Day 7, c) Day 10, d) Day14.

Differentiated cells were maintained in N2 medium with 10 µM SB431542. On day 20, expression of NC and POM marker gene expressions were assessed with qPCR. A three-fold increase in the expression of neural crest cell marker P75 was observed (Figure 13 a). More drastic increase in POM markers, FOXC1, PITX2, LMX1b, were observed (Figure 13 b and d). Expression of FGF10 was also assessed due to its vital role in LG development. We show that FGF10 is expressed in the RNA level in the differentiated POM (Figure 13 e).

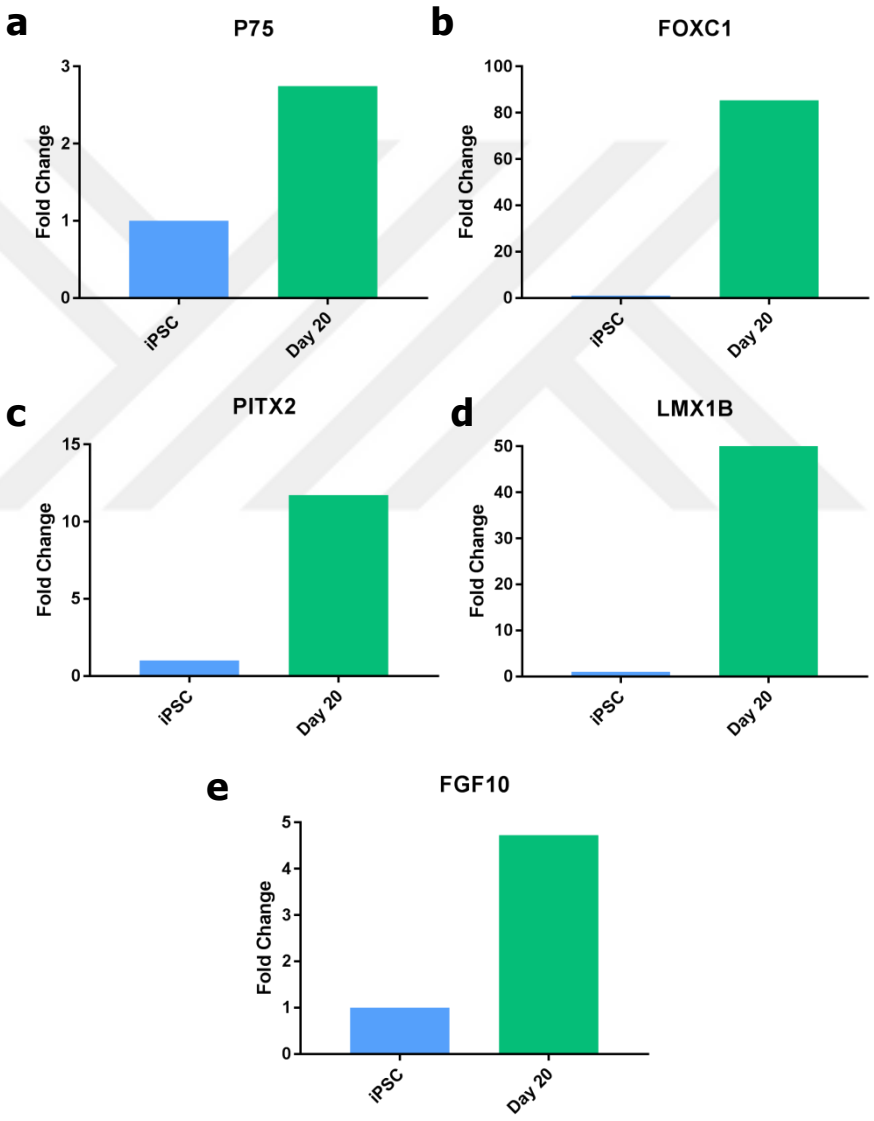

Figure 13 Expression of a) NC marker P75, b-d) POM markers FOXC1, PITX2 and LMX1b, e) FGF10 required for LG development. The expression levels are compared to expression levels in the pluripotent state. The values are normalized to GAPDH.

Differentiated cells were fixated on Day 14 and were stained against POM markers FOXC1 and PITX2, and cytoskeletal protein Actin, to visualize the cell morphology. Staining showed heterogeneous population with FOXC1 expression in dense areas, while PITX2 expression was observed only in big clumps (Figure 14 a and b). The cells do not look elongated although majority of the mesenchymal cells have elongated morphology when cultured *in vitro*.

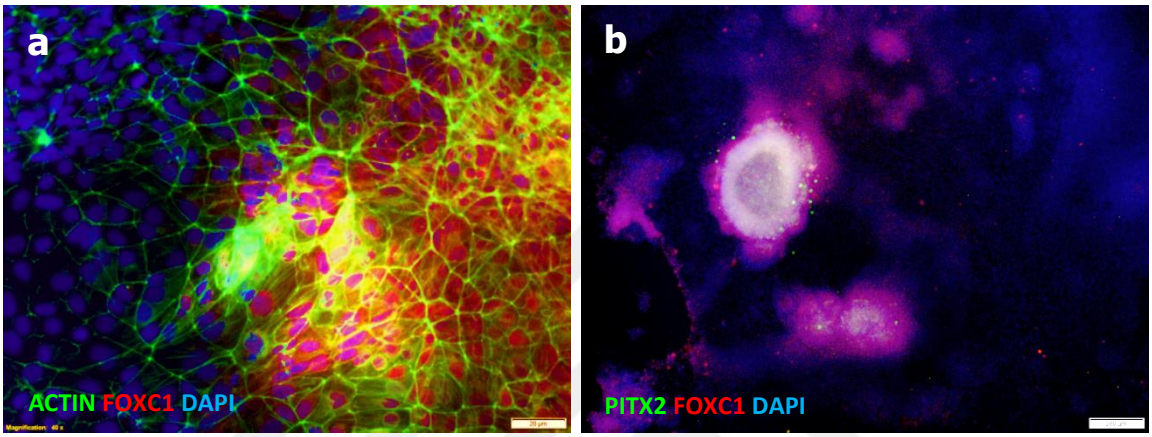

Figure 14 POM cells differentiated from hiPSCs on day 14 stained against a) Actin, FOXC1, b) FOXC1, PITX2. Nuclei are stained with DAPI.

The cells were dissociated and passaged on day 16 using Accutase and seeded on 1% Matrigel®. The cells did not adhere strongly and were dislodged even by gently moving the plate (Figure 15 a). The dislodged cells immediately formed clumps (Figure 15 b).

In order to overcome clumping, the cells were dissociated and passaged after 20 days of differentiating. The cells were seeded on 1% Matrigel® coated plates. Upon transferring $5.0x10^5$ cells to two wells of a 24 well plate, 2% Matrigel® solution was added, resulting in encapsulation of the cells. The following day, one of the wells was coated again with 2% Matrigel®. The cells were cultured for 8 additional days. Cells both with 1-layer coating (Figure 16 aand b) and 2-layer-coating adhered strongly and spread in the Matrigel® sandwich (Figure 16 c and d).

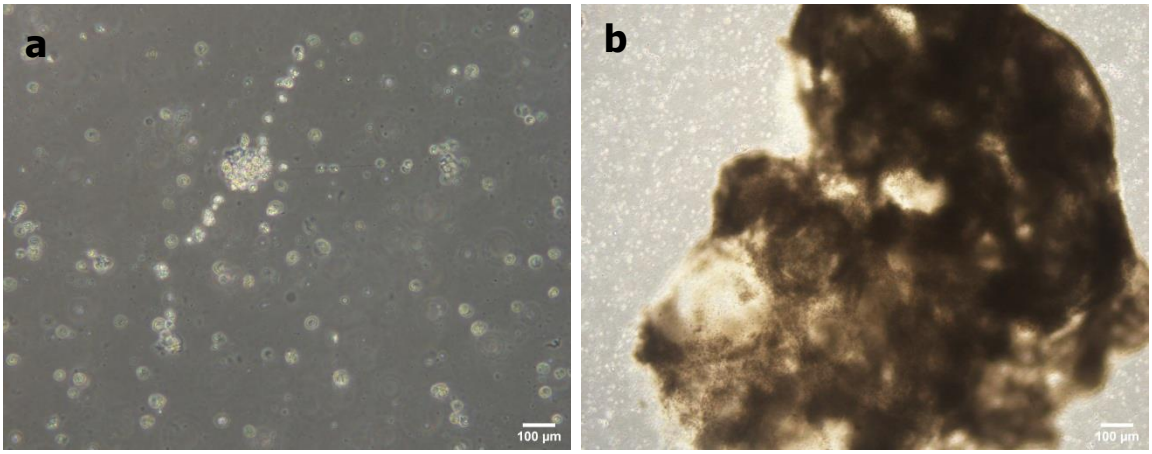

Figure 15 BF images of differentiated POM cells one day after passaging and seeding on Matrigel®, a) Cells weakly adhering or in suspension b) Clump formed by weakly adhering cells.

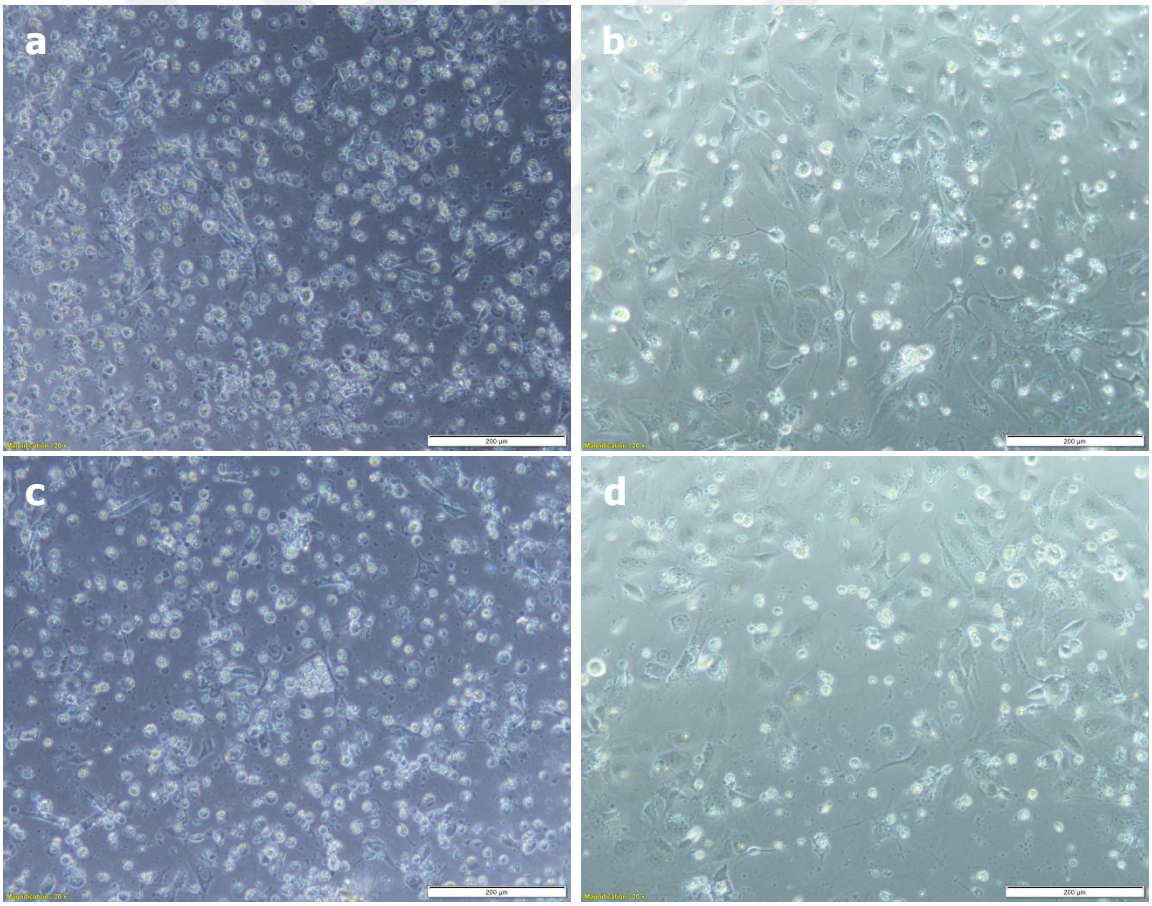

Figure 16 BF images of POM cells cultured in a 1 layer of Matrigel® sandwich on a) day 1 and b) day 8 and 2 layers of Matrigel® sandwich on c) day 1 and d) day 8.

After 8 days of culture, RNA was isolated from cells. Expression of POM related markers after 8 days in the Matrigel® culture system was compared with the RNA obtained the day of passaging. Dramatic decrease in the NC marker P75, POM markers FOXC1, PITX2 and LMX1b and FGF10 was shown,(Figure 17).

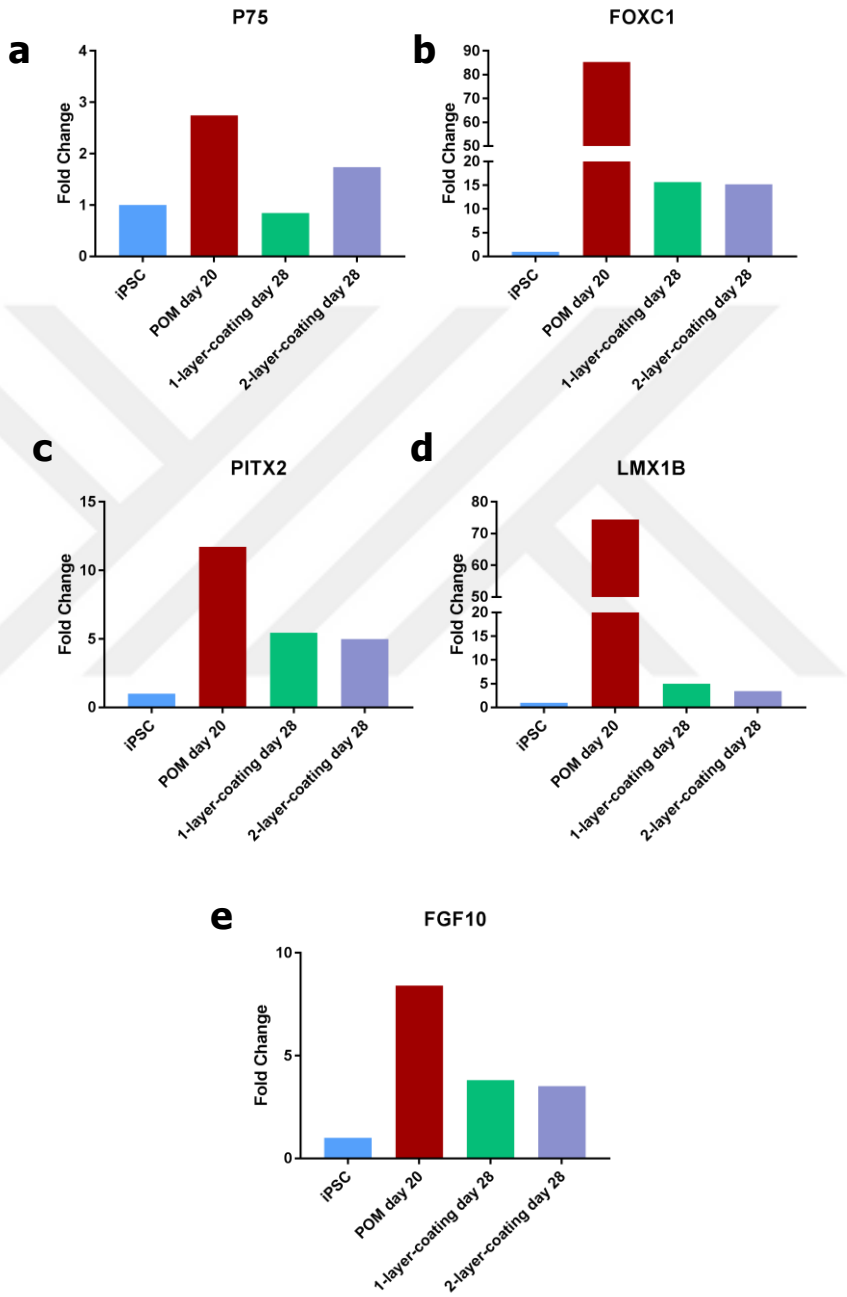

Figure 17 Expression of a) NC marker P75, b-d) POM markers FOXC1, PITX2 and LMX1b, e) FGF10 before passaging and 8 days after passaging either with 1-layer

coating or 2-layer coating. The expression levels are compared to expression levels in the pluripotent state. The values are normalized to GAPDH.

Overall, although POM marker expression was detected both in the RNA level and protein level, the cells could not be passaged to adhere without encapsulation. In the case of encapsulation with Matrigel®, the cells could not maintain their POM character and decrease in marker expression was observed. Therefore, this approach was not found convenient.

4.3. Formation of SEAM

After culturing 1500-4500 cells/well in a 6 well plate for 10 days in StemFit, the medium was changed to DM and cells were cultured for 25 days to induce SEAM formation. According to the protocol, SEAM should have formed until day 35. During the culture, the cells formed structures with cell heterogeneity, resembling zone formation (Figure 18 a). However, these structures started detaching from the laminin coated surface and started floating. By day 35, there were a few colonies still attached while the structures with so-called zones, and were floating (Figure 18 b-d). SEAM formation in the process of cornea organoid differentiation reported previously by Susaimanickam and colleagues led us to think that these colonies could be cornea organoids (Susaimanickam et al., 2017).

On day 35, the cells were harvested and RNA was isolated. According to the protocol, on day 35, OSE cells should have been present with PAX6 and P63 expression. Therefore, expressions of PAX6 and P63 were assessed through qPCR. PAX6 expression was found to be significantly increased (approximately 350-fold), confirming ocular cell differentiation (Figure 19 a). However, increase in P63 expression was not significant, around 1.5-fold, raising doubts about OSE differentiation (Figure 19 b) and their percentage in the culture.

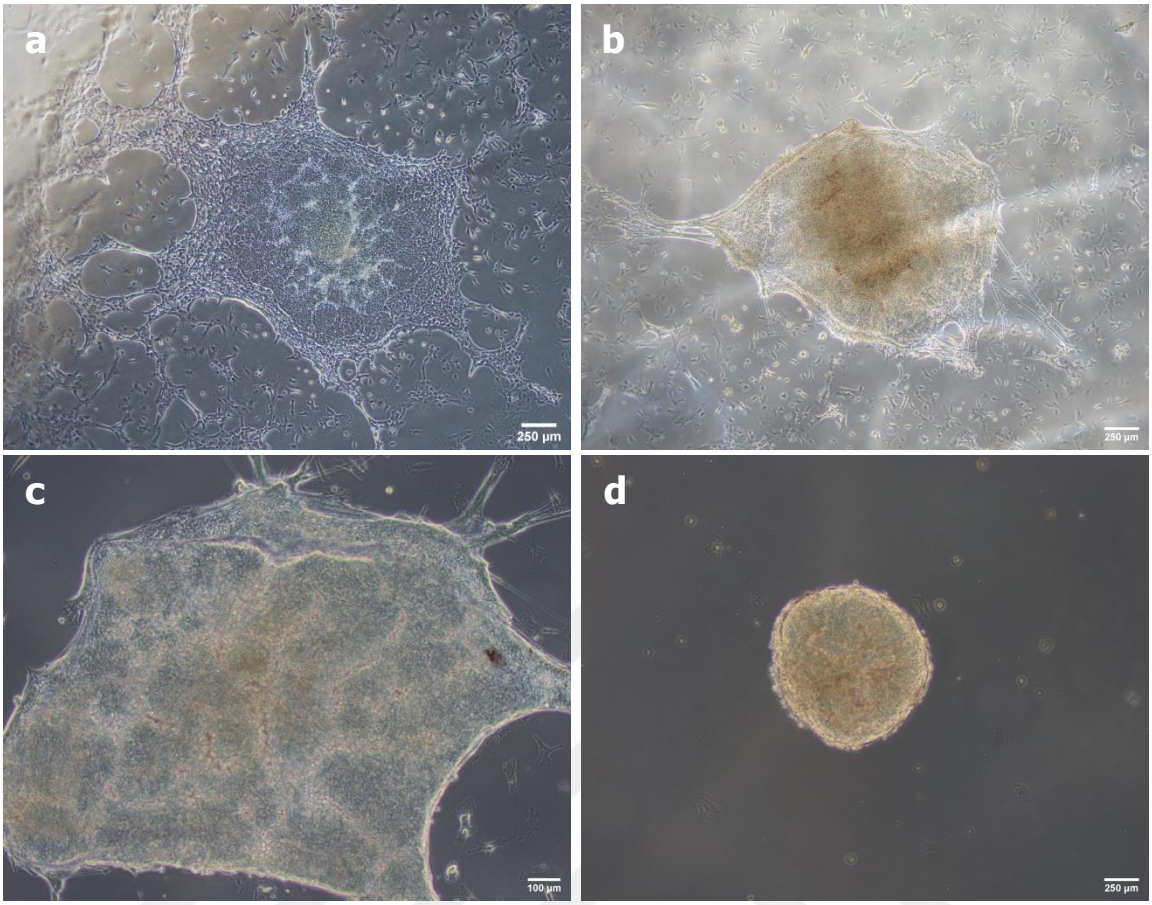

Figure 18 BF images of SEAM differentiation in a time course of 35 days. a) Colonies with areas resembling zones were observed around day 17. The colonies started detaching afterwards. Colonies with loose connections were observed on day b) 25 and c) 32 respectively d) while on day 35 some colonies were in suspension.

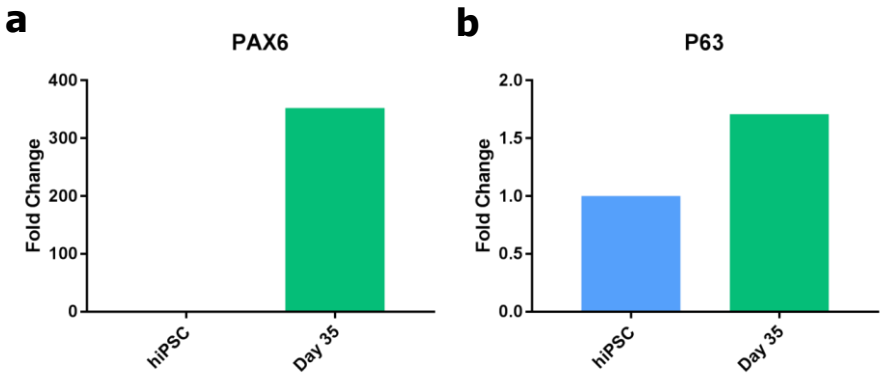

Figure 19 qPCR results of cells differentiated according to the SEAM protocol. Expression of OSE markers a) PAX6 and b) P63 are compared to expression levels in the pluripotent state. The values are normalized to GAPDH.

In order to examine ocular cell and OSE differentiation in the protein level, the cells were stained against PAX6 and TP63. Although heterogeneous, PAX6 protein was found to be present, suggesting the fact that cells differentiated into ocular cells (Figure 20 a). TP63 expression was also detected, however was not confined to a specific zone (Figure 20 b).

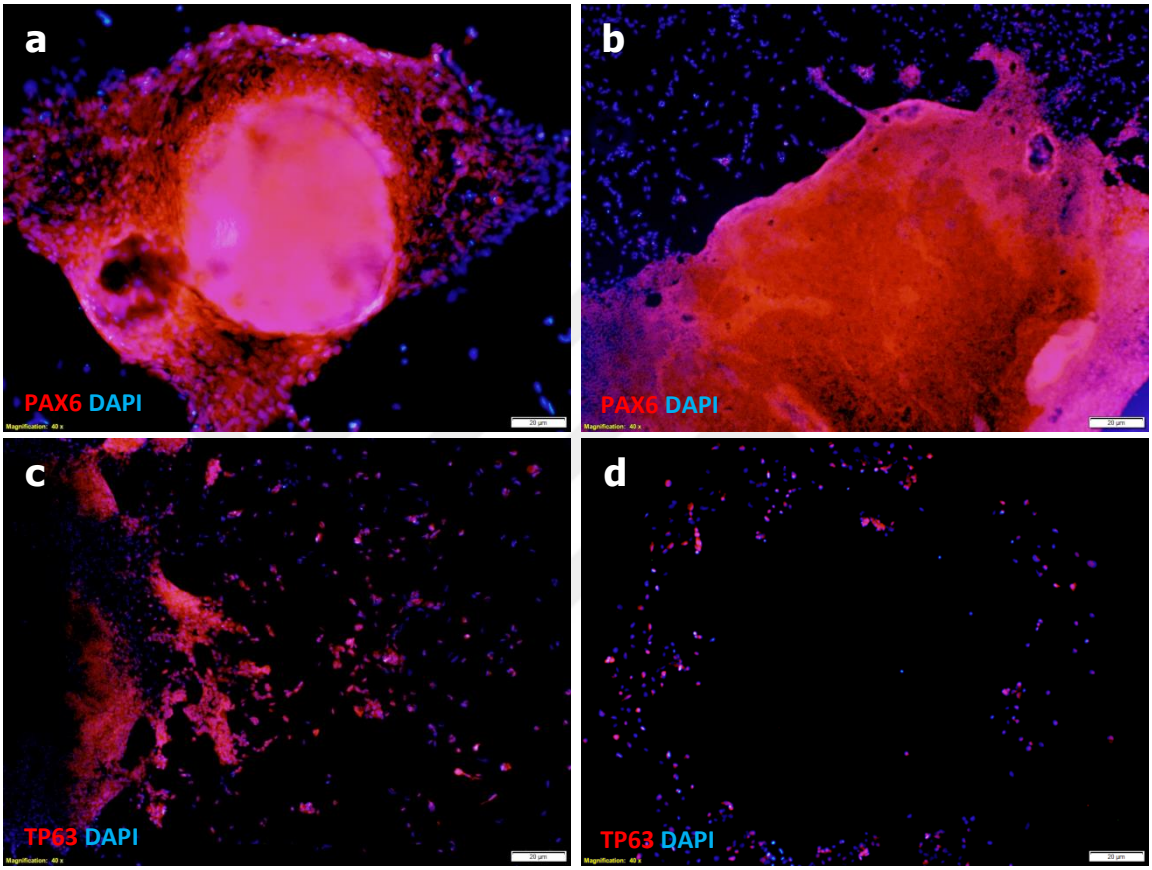

Figure 20 Cells differentiated according to the SEAM protocol on day 35 stained against a-b) PAX6 and c-d) TP63. Nuclei are stained with DAPI.

Although ocular cell differentiation was achieved through this protocol, the expected SEAMs with distinctive zones could not be observed on day 35. It is possible that with our cells the zone formation occurs much earlier (Figure 18 a). P63 expression was not significantly increased. These along with long culture time (35 days for OSE differentiation, additional 50 days for CE differentiation) and detachment of the colonies questioned the efficiency and reproducibility of this protocol.

4.4. Formation of MZOC

MZOCs were generated following the protocol explained in Section 3.6.2.3. The cells were maintained in ODM thereafter with daily medium changes. The colonies appeared encapsulated when first seeded; cells started spreading during the following days (Figure 21 a). The colonies appeared heterogeneous on day 5 with the spread cells maintaining different morphologies, resembling zone formation (Figure 21 b). From day 12 up until day 21, there were colonies with visible zones, the MZOCs (Figure 21 c and d).

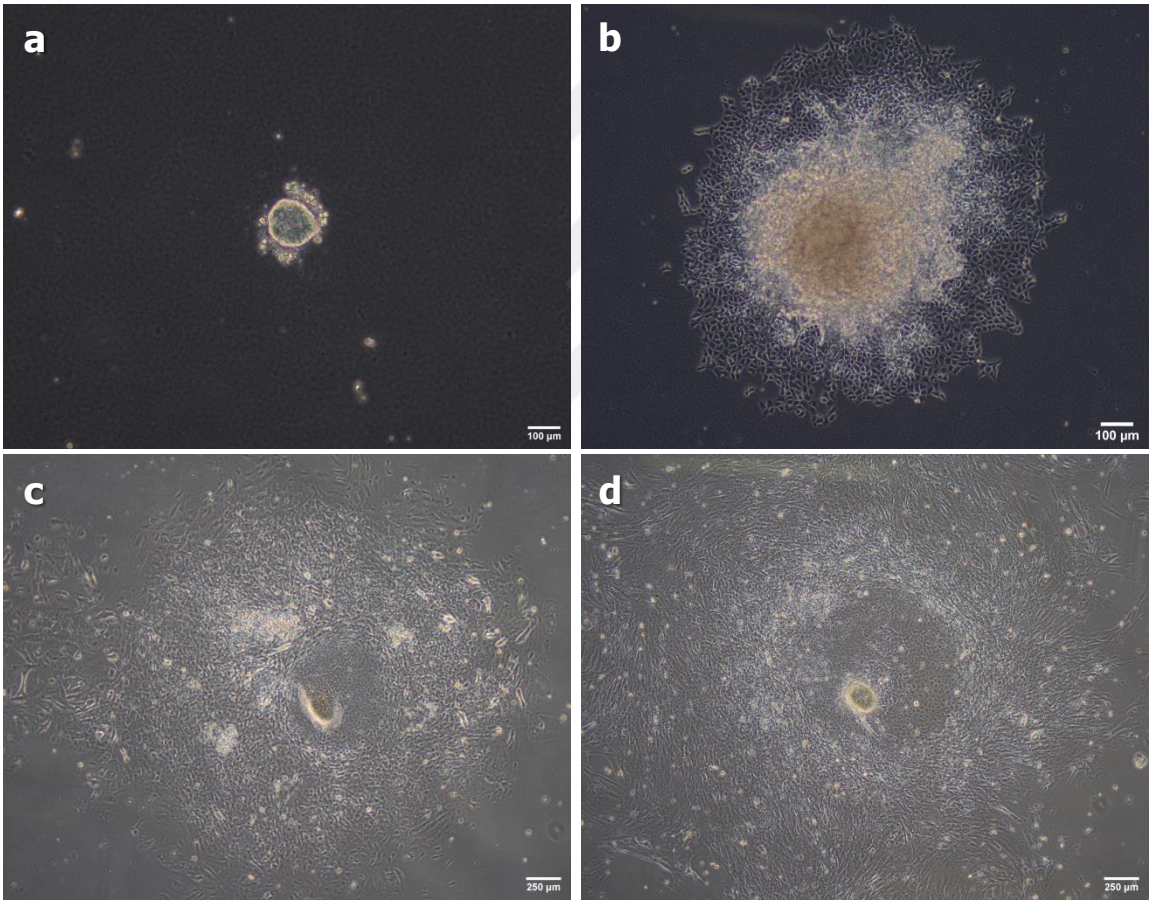

Figure 21 BF images MZOC formation a) 2.5D encapsulated colony on day 2 b) 2.5 D cultured colony showing spreading cells c) Spreading cells forming zones on day 12 d) Colony with distinct zones on day 19.

According to the protocol, emergence of zones is complete on day 21 and on the 3rd zone OSE cells should be present (Figure 22 a). In order to investigate that, RNA was isolated from cells on day 21 and expression of OSE markers PAX and P63 was assessed with qPCR. It was seen that expressions of both PAX6 and P63 significantly increased, with almost 200-fold and 900-fold respectively (Figure 22 b and c). This suggested that the cells differentiated into ocular lineages, and P63+ cell percentage was high.

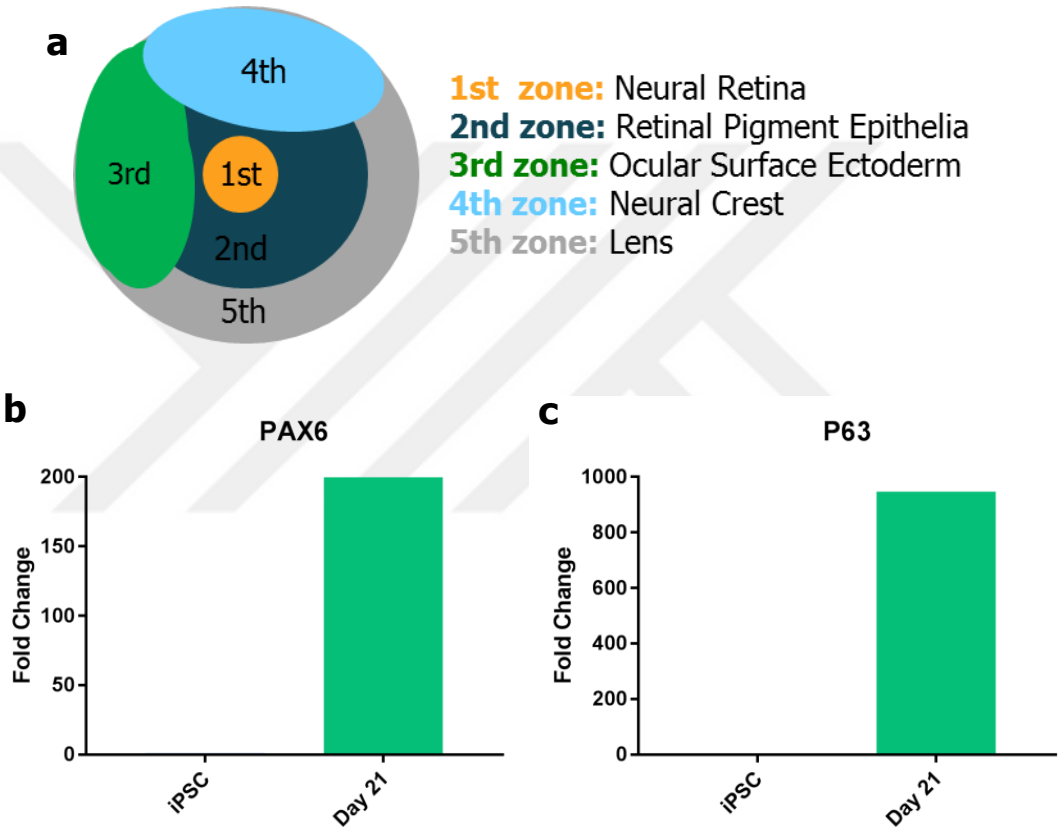

Figure 22 a) Cell types in each zone after 21 days of differentiation according to Li et al., 2019. b) The expression levels of OSE markers PAX6 and c) P63. Expression levels are compared to the pluripotent state. The values are normalized to GAPDH.

Expression of OSE and NC markers in the protein level was examined through ICC and IHC. According to the protocol, both cell types should be present in the MZOC in different zones (Figure 22 a). On day 21, PAX6+ and TP63+ cells were present in the suggested part of the colony, on zone 3 (Figure 23 a). In another colony, with less distinct zones, P75+ cells were visible, suggesting the presence of

NC cells (Figure 23 b). When the cells were further cultured in ODM, on day 35 PAX6+ and TP63+ OSE cells were detected through ICC (Figure 23 c). On day 45, P75+ and FOXC1+ NC/POM cells were present in the sectioned tissue (Figure 23 d). In the cryosections, cells were localized to from distinct structures, while some parts resembled sacs with hollow structures and cells aligned outside surrounding the hollow parts (Figure 23 c, d).

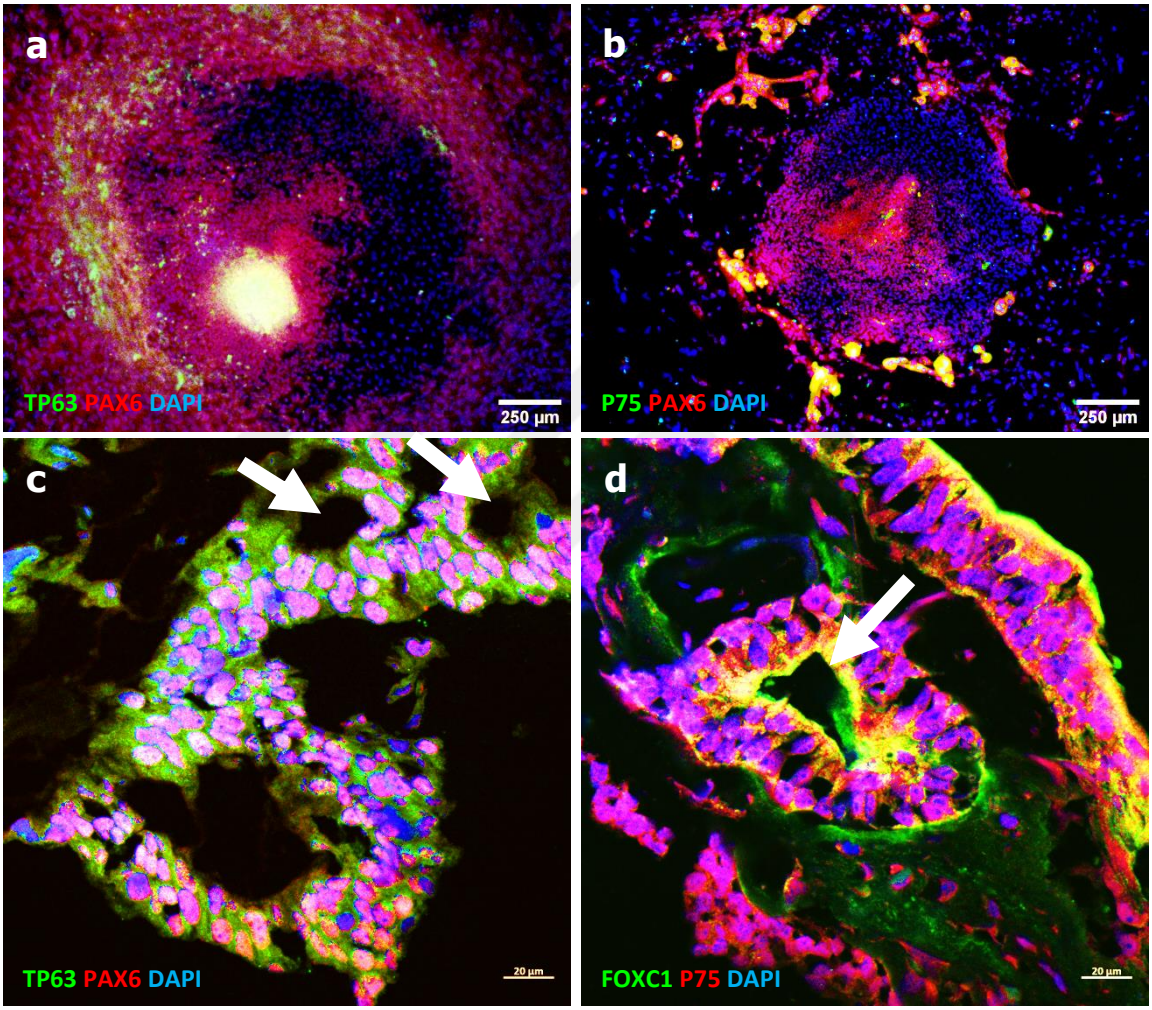

Figure 23 Expression of OSE and NC related markers in MZOCs. a) ICC on day 21 stained against OSE markers PAX6 and TP63 b) ICC on day 21 stained against NC marker P75 and PAX6 c) IHC on day 35 stained against OSE markers PAX6 and TP63 d) IHC on day 45 stained against NC marker P75, and FOXC1. Arrows indicate hollow structures. Nuclei are stained with DAPI.

OSE differentiation is important since LG epithelia arise from CE, which is derived from OSE. To assess the possibility of spontaneous differentiation of OSE into CE, the cells were stained against CE marker K13 and ocular marker PAX6. In the 3rd zone, PAX6+ and K13+ CE cells were observed (Figure 24 a,b). This suggested that the system had the ability to support spontaneous differentiation into CE and LG epithelia in a longer-term culture. On day 35, PAX6+ and K13+ cells were again present, in all layers of the colony with higher density of positive cells through the middle of the colony (Figure 24 c, d). Samples on day 35 of differentiation were sectioned and CE cells were again observed (Figure 24 e). On day 42 another culture was stained as a whole mount sample. K13+, TP63- cells, again suggesting CE presence were observed but differed from day 35 cells with their TP63 expression. That, along with different cell morphology raises questions about the ocular origin of these cells (Figure 24 f).

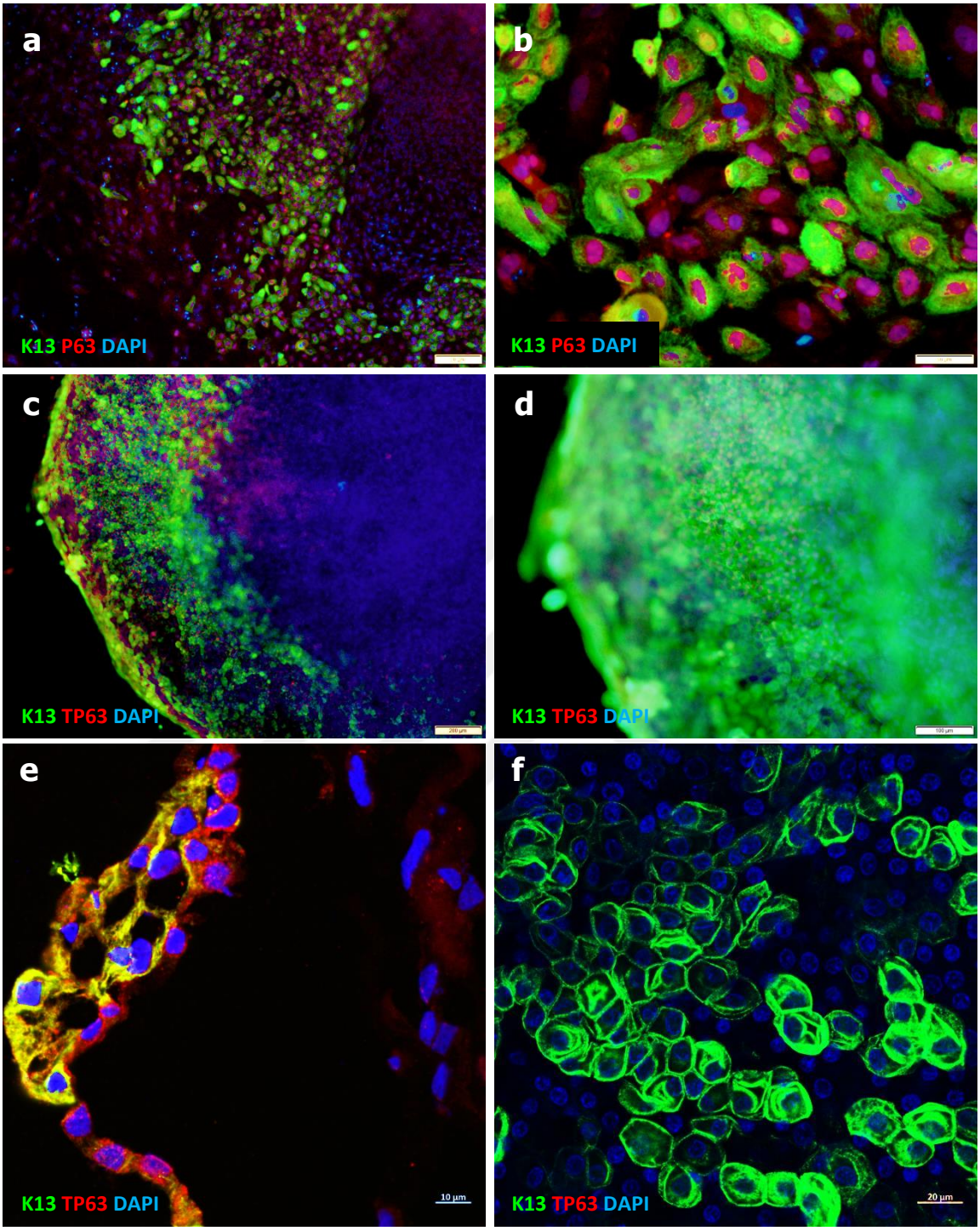

Figure 24 Differentiated cells stained against CE markers. a-b) ICC of day 21 stained against K13 and PAX6 c-d) ICC of day 35 stained against K13 and PAX6 e) IHC of day 35 cryosections stained against K13 and TP63 f) IHC of day 35 whole mount samples stained against K13 and TP63. Nuclei are stained with DAPI.

During the differentiation of hiPSCs, structures resembling LG were observed. One of these structures is shown in Figure 25. These structures often have parts resembling ducts. In most cases, these structures start forming near day 30 and keep developing (Figure 25 a). Spontaneous emergence of these LG-like structures is expected since MZOCs contain both cell types required for LG development, CE and POM. It is highly likely that this 2.5-dimensional (2.5D) culture system with all of the ocular cell types present offers the proper microenvironment to support spontaneous LG development.

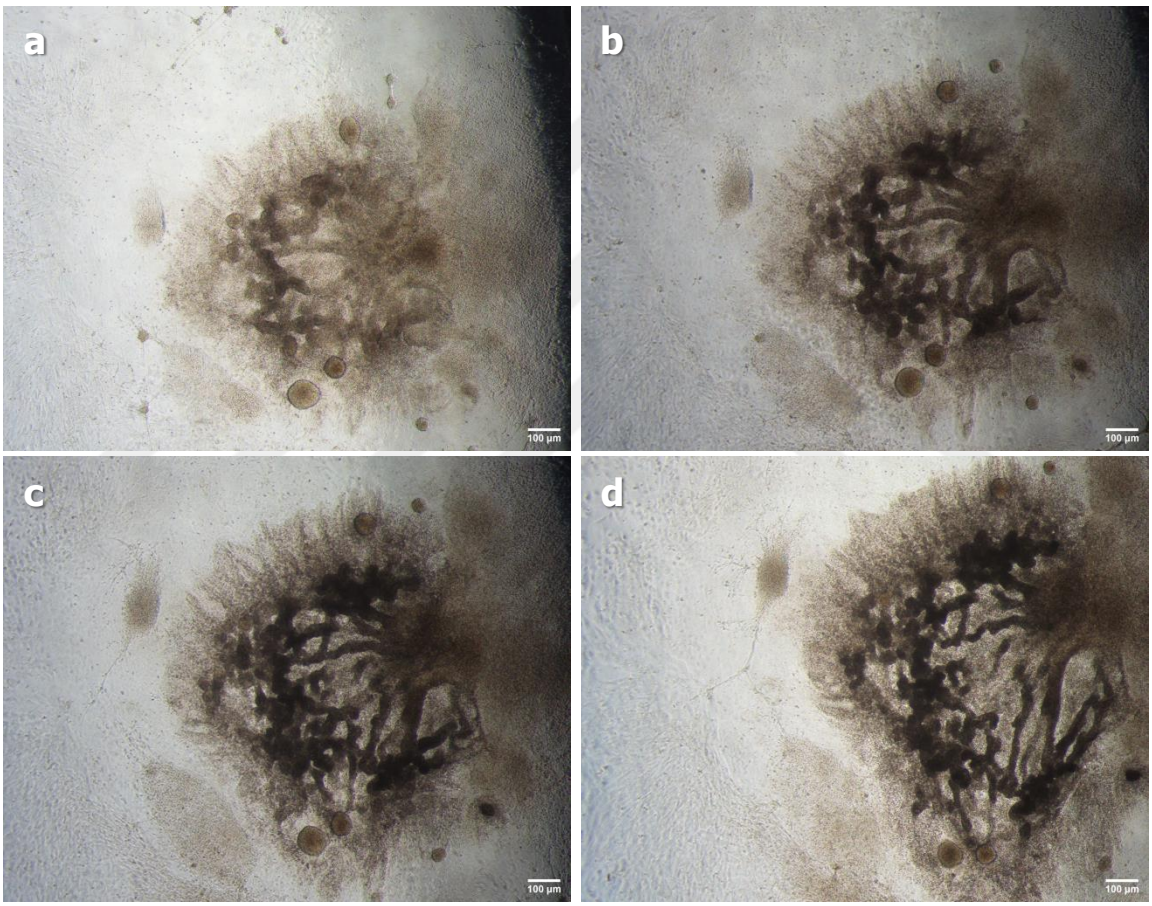

Figure 25 BF images of a spontaneously emerging structure resembling LG a) on day 29 b) on day 32 c) on day 35 d) on day 38.

MZOCs were cultured until day 120 and RNA was isolated on day 30 and day 120 to examine the LG related marker expressions in the RNA level. The CE marker K13 was found to be highly increased by day 30 (around 300-fold) and the expression level increased even further by day 120, up to almost 5000-fold (Figure

26 a). This can mean that CE cells had a higher proportion in the MZOC compared to other cell types. But it should be noted that K13 expression can also mean non-ocular epithelial cells as was suggested about TP63 negative cells in Figure 24 f. K15 is expressed in CE and is also considered to be the specific marker of developing LG epithelium (Hirayama et al., 2015). Increase in K15 expression was observed in day 30 with a 40-fold increase. Expression level was further increased by day 120 to up to 500-fold, suggesting a developing LG (Figure 26 b). K19 expression pattern is found to be parallel to K15 expression levels (Figure 26 c). K19 is another cytoskeletal protein expressed in the CE and is highly expressed in the developing LG and its expression decreases as the gland matures (Farmer et al., 2017).

M5AC is a type of mucin expressed by CE. Increase in the M5AC expression in day 30 was not detected, suggesting that the present CE cells were not functional yet and were not secreting. However M5AC expression significantly increased on day 120 (up to 20-fold) suggesting presence of mature and functional CE (Figure 26 d). AQP5 is a water channel that is considered to be the marker of LG acinar cells. LG secretions are excreted through these channels. AQP5 expression was detected on day 30 and was found to later decrease (Figure 26 e). This can be due to expression of the protein during early development of the gland. More samples are needed to assess this phenomenon's significance. The decrease in the expression levels can also be explained by CE overpopulation, which can also be supported by the dramatic increase in K13 expression. LYZ is one of the major components of LG secretion and its expression was found to be 80-fold increased on day 30. LYZ expression levels decreased in half in parallel to AQP5 expression by day 120, supporting the hypothesis of CE overpopulating (Figure 26 f).

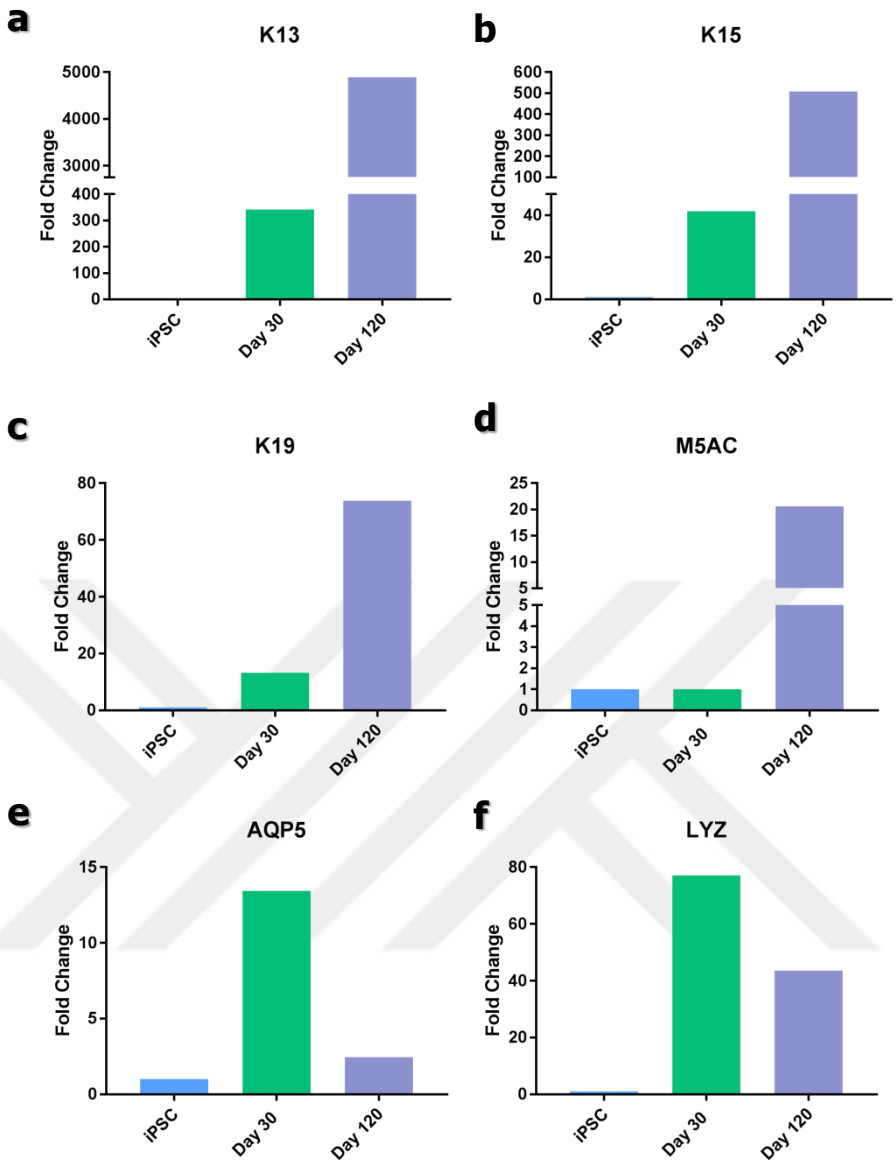

Figure 26 qPCR results of differentiated cells on day 30 and 120 of genes a) K13, b) K15, c) K19, d) M5AC, e) AQP5, f) LYZ. The expression levels are compared to expression levels in the pluripotent state. The values are normalized to GAPDH

The differentiated cells were fixated on day 35 to assess the protein expression in the aforementioned structures resembling the developing LG. FOXC1 is an important transcription factor for the development of the LG and is also expressed both in the LG epithelia and LG mesenchyme (Mattiske et al., 2006). IHC staining showed FOXC1 expression throughout the structure resembling acini. Calponin staining suggests the presence of myoepithelial cells (Figure 27 a). Although the cell type is not clear, N-cadherin is another protein expressed in the structures (Figure 27

b). As mentioned earlier, K15 is a type of cytokeratin that is accepted to be a marker of the developing LG epithelia. K15 was widely expressed along with FOXC1 in these structures (Figure 27 c). This along with the shape of the structures support that these are developing LGs. More importantly, the cells expressed the LG acini marker AQP5, and Na^+/K^+ ATPase, which is also expressed in LG acini (Okami et al., 1992) (Figure 27 d).

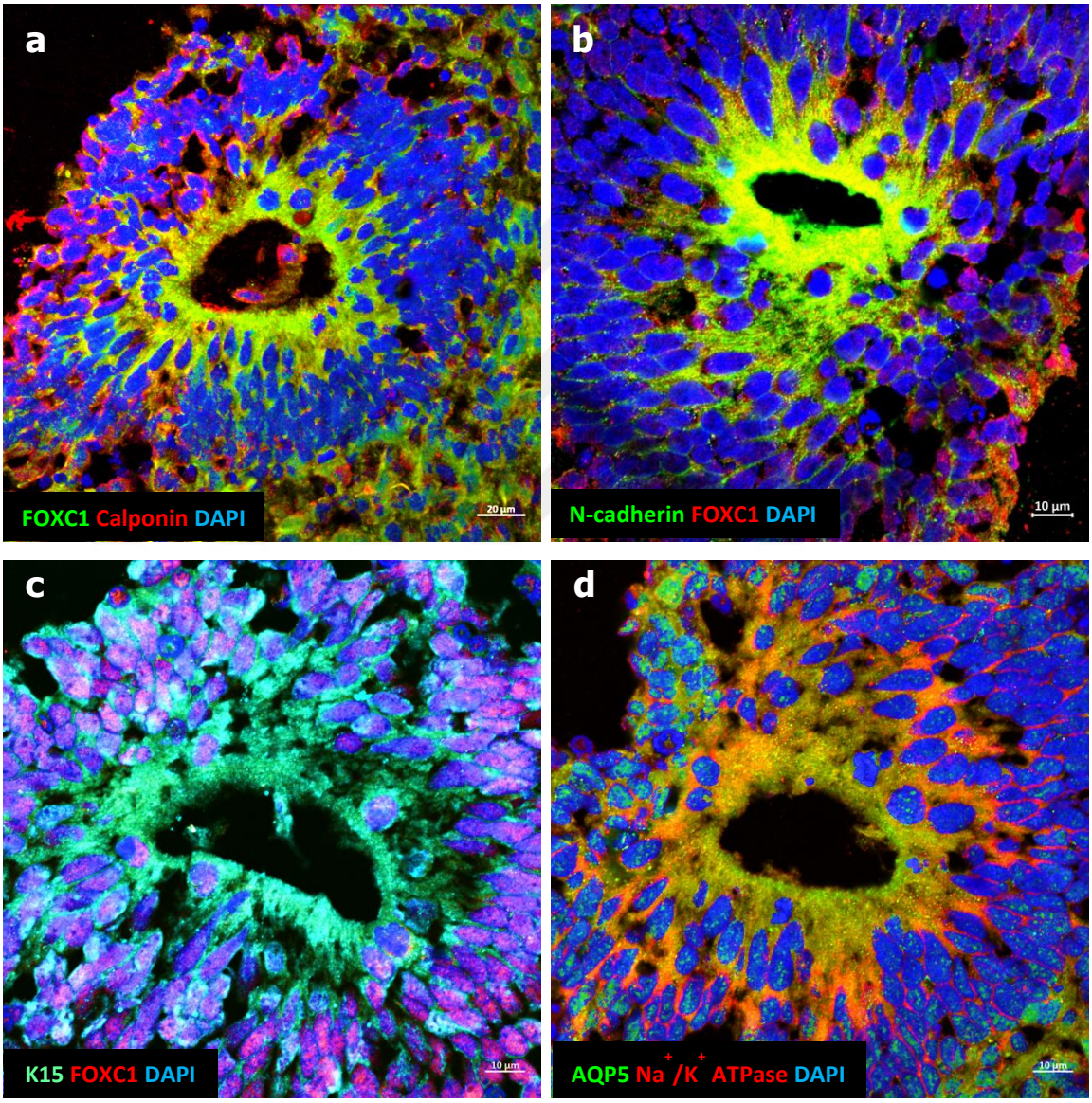

Figure 27 IHC of cryosectioned 35-day old structures resembling LG, stained against a) FOXC1 and Calponin b) N-cadherin and FOXC1 c) K15 and FOXC1 d) AQP5 and N^+/K^+ ATPase. Nuclei are stained with DAPI.

The findings suggesting that the structures are truly LG raised the question whether they were functional in terms of secretion. In order to assess that, a 42-day old culture was induced with 10μM forskolin. Medium was collected in different time intervals to assess the accumulated lactoferrin level in the medium. The results are shown in Figure 28, implying that the cultures are capable of tear secretion when stimulated, thus confirming that the culture system had functional LG structures.

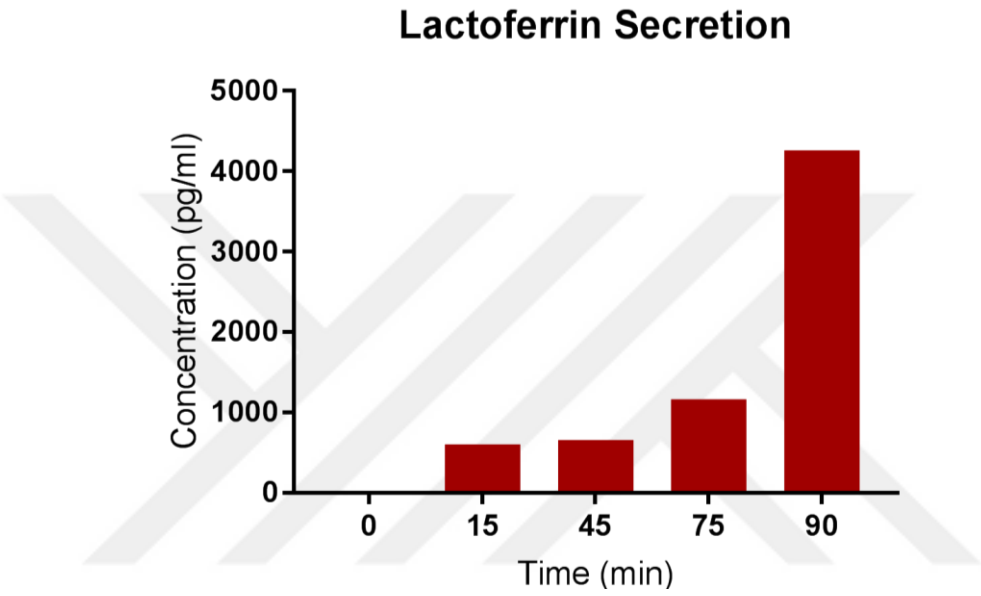

Figure 28 Human lactoferrin secretion ELISA results of 42-day old MZOC cultures

Heterogeneity of the culture systems was an expected finding. This is because the MZOCs differentiate into all of the ocular cell types; neural retina, retinal pigment epithelia, OSE, NC and lens. While the coexistence of NC and OSE leads to spontaneous LG development, the other cell types also gives rise to more mature types, and differentiate to form retina, cornea, neurons, lens etc. In order to be able to collect pure tear, cell types other than LG must be dismissed from the culture.

In order to purify the culture system, our first approach was to sort out CE combine them POM obtained via POM differentiation. However, CE does not express any known surface markers suitable for FACS. According to Hayashi and colleagues, corneal epithelial cells can be identified via co-expression of SSEA4 and ITGB4. They also identified SSEA4-, ITGB4+ cells as CE (Hayashi et al., 2016). To analyze the

differentiated cells according to this approach, 21, 30 and 35 days old cells were stained against SSEA4 and ITGB4 to be analyzed in FC. According to that article, Q1 should represent CE population and Q2 should show the corneal epithelial cells (Hayashi et al., 2016). FC results showed increasing Q1 population parallel to time. On the other hand, in the Q2 region there was not a significant population before day 35 (Figure 29).

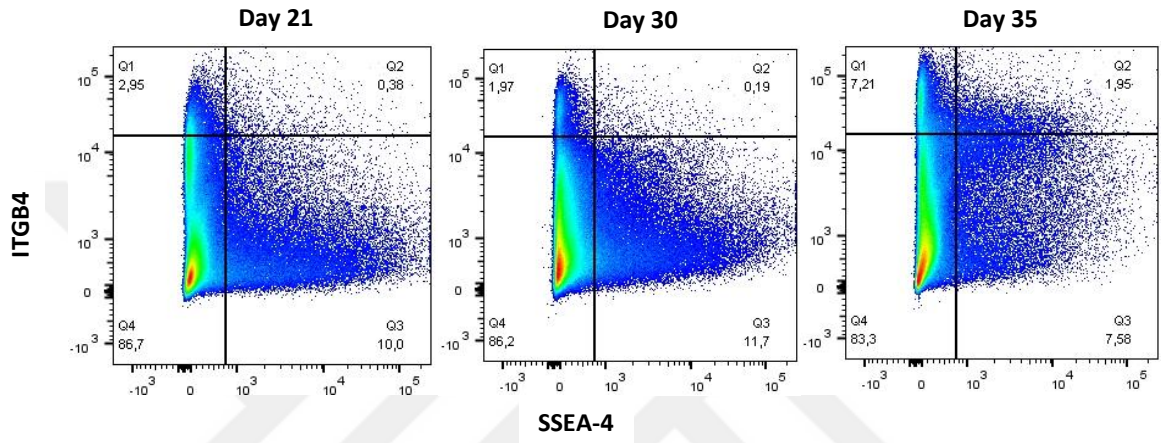

Figure 29 FC analysis results of 21, 30 and 35 days old MZOC differentiation cultures. Q1 depicts the ITGB4+ SSEA4- population. Q2 depicts the double positive (ITGB4+ SSEA4+) population.

In order to check whether the cells in Q1 are really CE, the obtained cells were sorted through FACS and were cultured in ODM on a Matrigel® coated plate for 70 days. The fixated samples were stained against the corneal epithelial marker K12 and CE marker K13. The results showed that the cells expressed the corneal epithelial marker K12 and not the CE marker K13 (Figure 30). It was expected to have K13+ CE cells according to the literature. This revealed that the approach Hayashi et al., 2016 adopted may not be applied to our system (Hayashi et al., 2016).

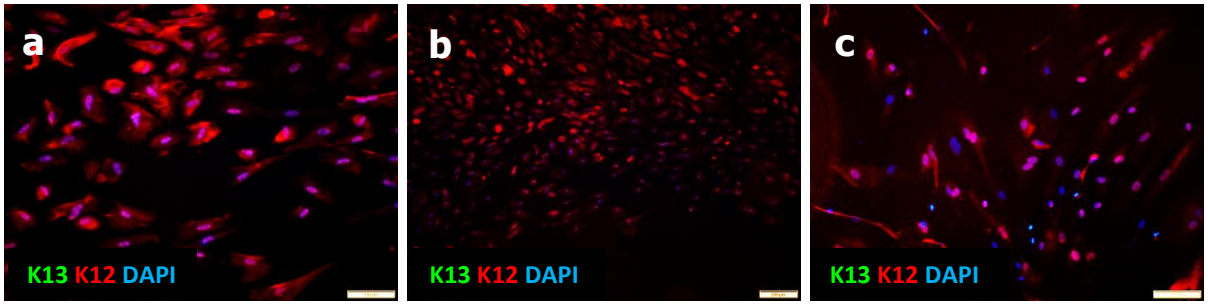

Figure 30 SSEA4- ITGB4+ cells obtained via FACS were cultured for 70 days and stained against cornea epithelial marker K12 and CE marker K13. a) ICC of cells sorted on day 21 b) ICC of cells sorted on day 30 c) ICC of cells sorted on day 35. Nuclei are stained with DAPI.

Overall, the approach consisting generation of MZOCs to obtain LG cells proved to be successful and functional cells capable of tear secretion were obtained.

4.5. IHC of Mice LG

In order to examine the developing tissue before inducing its development *in vitro*, LG tissue obtained previously from E16.5 C57BL/6 mice was stained against LG precursor cells markers. The tissue was embedded in OCT and was cryosectioned.

PAX6 staining confirmed that the tissue had arisen from eye field cells. PAX6 along with K13 staining revealed CE cells present in the edge of the tissue (Figure 31 a). FOXC1 and PITX2 staining showed presence of POM cells in the tissue (Figure 31 b). P75 staining revealed NC cells, adjacent to FOXC1 expressing cells (Figure 31 c). This is probably due to the fact that POM is derived from NC cells. FOXC1 and PAX6 staining supported presence of the developing LG (Figure 31 d). As mentioned earlier, the gland develops as a result of interactions between CE and POM. The presence of these precursor cell types revealed that the gland was still developing.

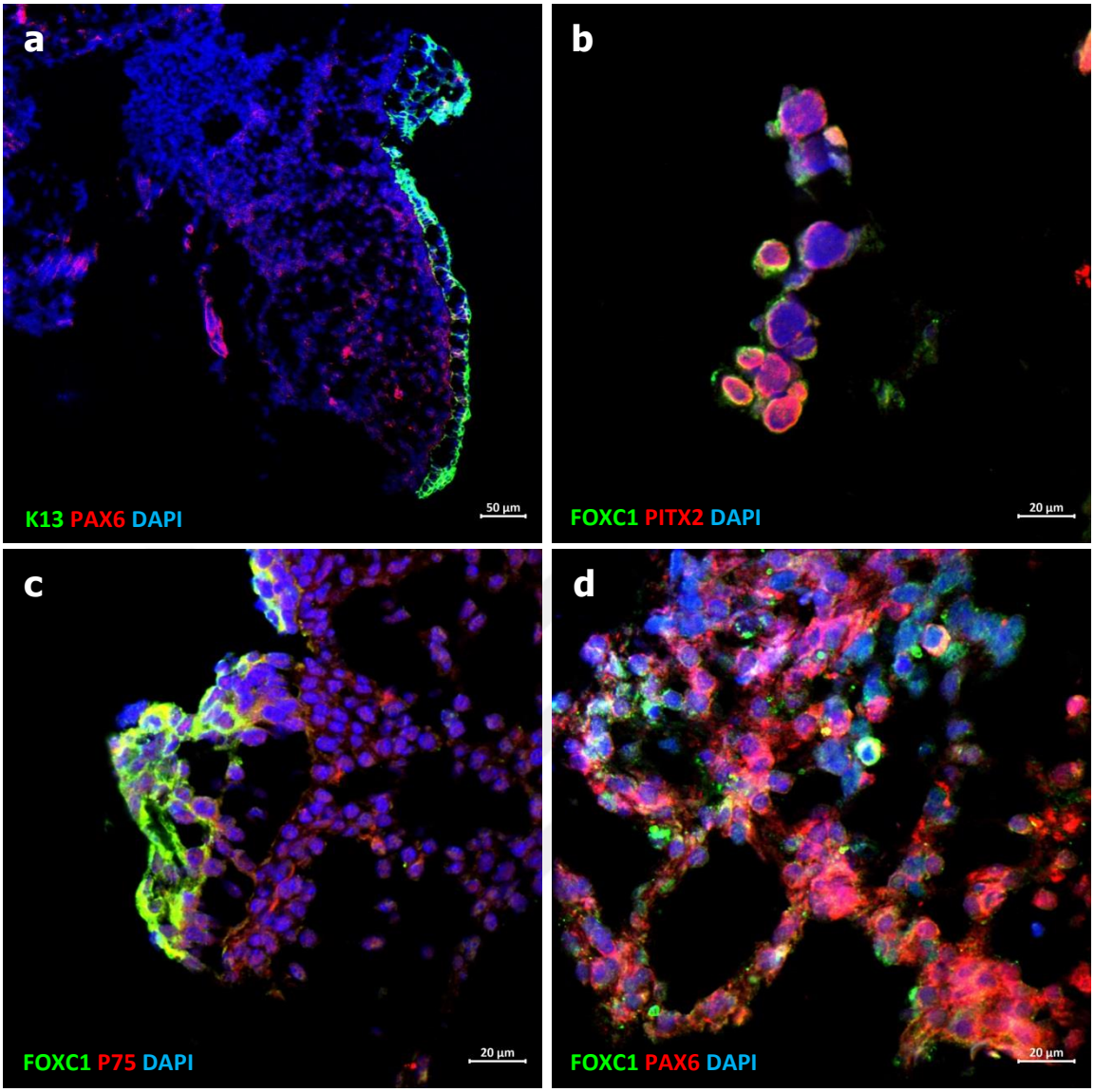

Figure 31 E16.5 mice cryosections stained against markers of LG precursor cells. a) Section stained against K13 and PAX6 suggesting CE cell presence b) Section stained against FOXC1 and PITX2 suggesting POM presence c) FOXC1 and P75 stained section suggesting presence of NC cells d) Presumptive developing LG stained against FOXC1 and PAX6. Nuclei are stained with DAPI.

5. DISCUSSION

In this thesis, different eye-field cell differentiation methods were investigated to develop an approach for generation of a LG construct from hiPSCs. The methods were compared for their efficiencies in differentiation according to marker expression levels. Among the three protocols, only the MZOC approach proved to be successful and prolonging the MZOC culture resulted in formation of a functional LG mimicry.

To our knowledge, the only published research investigating LG epithelial differentiation from pluripotent cells was conducted by Hirayama and colleagues (Hirayama et al., 2017). Although differentiation of human embryonic stem cells (hESC) into LG epithelial cells with the overexpression of the transcription factors involved in the organogenesis of mice LG is promising in its nature, there are some burdens associated with it. Firstly, mice and human LG development differs in some aspects, and although it is hard to find material, microarray analysis of the human embryonic LG is required to identify the transcription factors. Secondly, hiPSCs remains a much more flexible option than hESCs, and differences between hiPSC and hESCs can affect the results of this differentiation protocol. Thirdly, overexpression of the transcription factors is a rather "artificial" method to differentiate cells, utilization of growth factors and tailoring the ECM would aid in the maturation of the gland. Fourthly, the functionality of these cells was not assessed in terms of secretion, and the maturity of these cells is not well addressed. Finally, the native LG is composed of both mesenchymal and epithelial cells, and even though the epithelial cells possess the main secretory function, in order to construct a fully functional and mature gland, utilization of iPSCs and co-differentiating these cells into both epithelial and mesenchymal cells is a more promising approach.

5.1. POM Differentiation

The cells differentiated using inhibitors for WNT and TGFβ pathways showed FOXC1 and PITX2 expression in the RNA level, and heterogeneous expression in the protein level. The culture gave rise to monolayer of POM-like cells (Figures 12-14). However when passaged, the cells could not be maintained on a Matrigel® coated

plate (Figure 15) and when cultured in a Matrigel® sandwich with medium changes every other day, expression of marker genes decreased (Figures 16, 17).

The loss in marker expression can be attributed to passaging itself, or to the difference between 2D and 3D culturing. In 3D cell culture; nutrient, differentiation factors and oxygen need to diffuse through the gel. This often results in gradient formation and possibly hypoxic regions, which stimulate the cells to further differentiate. This problem about the character loss in case of encapsulation posed a major problem for our system.

The biggest burden about this approach is that the regime of inhibitor application after the differentiation period (14 days) is not clear (Lovatt et al., 2018). Moreover, the level of matureness of the cells is not clear. In the literature, the cells were labeled as "NC cells expressing POM markers" (Lovatt et al., 2018). Cells obtained in this thesis were shown to express FGF10, the growth factor required for LG formation (Figure 13 e). However the presence of the protein could not be investigated in the protein level.

In this thesis, the cells obtained via this protocol were planned to be combined with the CE cells obtained via other protocols. Through the FGF10 produced by POM, the interaction between cells could potentially give rise to LG. However the question of when to combine the cells and the possible different maturation levels of respective cells come out as other problems of the employment of this method.

5.2. SEAM Differentiation

35 days of SEAM differentiation protocol did not result in formation of SEAMs. However, through PAX6 expression analysis, it was confirmed that the cells differentiated into ocular cells (Figures 19 a, 20 a, b). Emergence of floating colonies hindered the efficiency of the protocol since removal of non-epithelial cells through manual pipetting would not be applicable (Figure 18).

This can be due to various reasons. The most probable reason is the variance between hiPSCs obtained from different sources. Even in the protocol paper, it was

stated that this protocol did not work with some hiPSC lines and it was recommended to use 201B7 (ATCC® ACS-1023). The protocol can be optimized for each hiPSC line however, like the authors of the paper, we did not work on further optimizing the protocol (Hayashi et al., 2017).

Another drawback of the protocol is the culture time required to obtain OSE cells (approximately 35 days) and CE cells (at least 75 days) (Hayashi et al., 2016). While in the MZOC protocol, OSE along with CE cells can be obtained after day 21 of differentiation (Li et al., 2019).

Use of a matrix, iMatrix-511, that is less employed in hiPSC studies compared to Matrigel® was one of the complications of the protocol. Although it was shown that use of different types of Laminin can selectively support differentiation of hiPSCs into ocular lineages, adaptation of hiPSCs cultured on Matigel with mTeSR1 requires at least 3-4 weeks prior to induction of differentiation, making the differentiation protocol even longer (Hayashi et al., 2017; Shibata et al., 2018).

5.3. MZOC Differentiation

According to the MZOC differentiation protocol, hiPSCs cultured in 2% Matrigel®-mixed EDM for 2 days differentiate into anterior neuroectoderm (Li et al., 2019). We did not investigate the anterior neuroectoderm associated markers, however later observed zone formation. According to the protocol, by day 21, 5 zones are observed corresponding to neural retina, RPE, surface ectoderm, NC, and lens. The zones have boundaries and differences between cell types were visible. Among the zones, zone 3 constitutes OSE cells, the ancestors of CE required for LG formation. In addition to this, zone 4 houses NC cells which can differentiate into POM required for LG development (Li et al., 2019).

In this study, by following the protocol by Li et al., 2019 we were able to verify OSE differentiation (Figure 23 a, c). We observed that by extending the culture time, CE and POM cells could be formed (Figure 23 d, Figure 24). And co-presence of CE and POM cells spontaneously gave rise to LG-like constructs (Figure 25). By analyzing

the constructs we were able to show that the constructs were functional LG organoids (Figures 27, 28).

Success of this protocol can be attributed to the provided microenvironment. With this protocol, we were able to see formation of 3D structures, and other functional cell types (pigment secreting cells). This is potentially triggered by the coexistence of all of the ocular cell types. Although LG formation does not require presence of an optic cup, synchronized development of POM and CE cells probably leads to spontaneous interaction that leads to LG formation.

SEAM method is similar to MZOC method as they both give rise to structures with zones mimicking eye development. MZOC differentiation differs from SEAM differentiation by containing five zones in comparison to four zones, and by being 2.5 D. In 2D SEAM culture equal amount of nutrients reach the cells as opposed to natural developmental process. 2D culture therefore fails to mimic the physiology of native tissues. The 2.5 D culture accelerates the differentiation process dramatically. In this system although the cells are grown adhered to the plate, they still form spheroids.

FACS results did not show the expected colony characters. This can be due to numerous reasons. First, in the SEAM method, the culture system is purified with manual pipetting prior to FACS. This approach was not applicable in the MZOC system, since the cells are coated with Matrigel® and cannot be detached from the surface with pipetting. Secondly, after day 21, the cells rapidly form 3D structures, which are difficult to disintegrate. Even after enzyme treatment is carried out as explained in Section 3.6.3.8, the structures do not fully dissociate. Thus, the obtained cell number is almost always lower than the real number of cells in the culture. Moreover, extended enzyme treatment results in more dead cells. The characteristic of the intact cells are not known since they cannot be analyzed with flow cytometry. Perhaps, these cells have epithelial origin and the fact that they cannot be disintegrated affects the populations currently analyzed.

Overall, after confirming the OSE development in MZOCs, the colonies were further kept in ODM for a prolonged period. This allowed the probable interactions between the NC derived POM and OSE derived CE to give rise to LG tissue. The constructs were proven to be functional in terms of tear secretion after being stimulated with forskolin.

6. CONCLUSION AND FUTURE DIRECTIONS

In conclusion, in this study successful differentiation of hiPSCs into a functional LG construct is reported for the first time in the literature. The differentiated constructs offer a potential source to study LG development and pathology, as well as can act as a platform for drug testing. Secretion of the constructs can be used to replace artificial tears in a patient-specific manner for the treatment of. The only possible burden associated with the use of the secretion is the other components present in the culture system.

Although the differentiation method spontaneously gives rise to functional LG tissue, other ocular tissues develop along with it. Differentiation protocol should therefore be optimized further to obtain a construct with a less number of undesired cell types. FACS can be a viable choice for purifying the tissues, and can be applied either before LG formation, to sort out CE and POM cells, or after LG development to sort out the differentiated functional cells.

In order to appropriately recapitulate the human LG, a bioengineered microenvironment should be provided. The LG construct can possibly be generated by encapsulating the sorted cells in a synthetic hydrogel. Thus the system can be converted to be animal-free by using the hydrogel instead of Matrigel®. Through use of photocrosslinkable hydrogels, preferred patterns can be formed.

Generation of the construct can be transferred to a dynamic environment to better recapitulate the conditions of the developing gland. Culturing the developed LG inside a microfluidic system can offer the advantages of culturing the various cells of the LG by feeding with different media, and the secretion can be collected from the outlet of the system.

7. REFERENCES

1. Buckley RJ. Assessment and management of dry eye disease. Eye (Lond). 2018;322: 200-3.

2. Conrady CD, Joos ZP, Patel BC. Review: The Lacrimal Gland and Its Role in Dry Eye. J Ophthalmol. 2016;2016: 7542929.

3. Bron AJ, de Paiva CS, Chauhan SK, Bonini S, Gabison EE, Jain S, et al. TFOS DEWS II pathophysiology report. Ocul Surf. 2017;153: 438-510.

4. Hirayama M, Tsubota K, Tsuji T. Bioengineered Lacrimal Gland Organ Regeneration in Vivo. J Funct Biomater. 2015;63: 634-49.

5. Villatoro AJ, Fernandez V, Claros S, Alcoholado C, Cifuentes M, Merayo-Lloves J, et al. Regenerative Therapies in Dry Eye Disease: From Growth Factors to Cell Therapy. Int J Mol Sci. 2017;1811.

6. Takahashi K, Tanabe K, Ohnuki M, Narita M, Ichisaka T, Tomoda K, et al. Induction of pluripotent stem cells from adult human fibroblasts by defined factors. Cell. 2007;1315: 861-72.

7. Yamanaka S. Induced Pluripotent Stem Cells: Past, Present, and Future. Cell Stem Cell. 2012;106: 678-84.

8. Asal M, Güven S. 7 - Stem cells: sources, properties, and cell types. In: Vrana NE, Knopf-Marques H, Barthes J, editors. Biomaterials for Organ and Tissue Regeneration: Woodhead Publishing; 2020. p. 177-96.

9. Örge FH, Boente CS. The Lacrimal System. Pediatr Clin North Am. 2014;613: 529-39.

10. Garg A, Zhang X. Lacrimal gland development: From signaling interactions to regenerative medicine. Dev Dyn. 2017;24612: 970-80.

11. Paulsen FP, Berry MS. Mucins and TFF peptides of the tear film and lacrimal apparatus. Prog Histochem Cytochem. 2006;411: 1-53.

12. Tsubota K. Tear dynamics and dry eye. Prog Retin Eye Res. 1998;174: 565-96.

13. Rocha EM, Alves M, Rios JD, Dartt DA. The Aging Lacrimal Gland: Changes in Structure and Function. The Ocular Surface. 2008;64: 162-74.

14. Selvam S, Thomas PB, Gukasyan HJ, Yu AS, Stevenson D, Trousdale MD, et al. Transepithelial bioelectrical properties of rabbit acinar cell monolayers on polyester membrane scaffolds. American Journal of Physiology-Cell Physiology. 2007;2934: C1412-C9.

15. Swindell EC, Liu C, Shah R, Smith AN, Lang RA, Jamrich M. Eye formation in the absence of retina. Dev Biol. 2008;3221: 56-64.

16. Dean C, Ito M, Makarenkova HP, Faber SC, Lang RA. Bmp7 regulates branching morphogenesis of the lacrimal gland by promoting mesenchymal proliferation and condensation. Development. 2004;13117: 4155.

17. Makarenkova H, Ito M, Govindarajan V, Faber S, Sun L, McMahon G, et al. FGF10 is an inducer and Pax6 a competence factor for lacrimal gland development. Development (Cambridge, England). 2000;127: 2563-72.

18. Qu X, Pan Y, Carbe C, Powers A, Grobe K, Zhang X. Glycosaminoglycan-dependent restriction of FGF diffusion is necessary for lacrimal gland development. Development. 2012;13915: 2730.

19. Tsau C, Ito M, Gromova A, Hoffman MP, Meech R, Makarenkova HP. Barx2 and Fgf10 regulate ocular glands branching morphogenesis by controlling extracellular matrix remodeling. Development. 2011;13815: 3307.

20. Pan Y, Carbe C, Powers A, Zhang EE, Esko JD, Grobe K, et al. Bud specific N-sulfation of heparan sulfate regulates Shp2-dependent FGF signaling during lacrimal gland induction. Development. 2008;1352: 301.

21. Gayton JL. Etiology, prevalence, and treatment of dry eye disease. Clin Ophthalmol. 2009;3: 405-12.

22. Phadatare SP, Momin M, Nighojkar P, Askarkar S, Singh KK. A Comprehensive Review on Dry Eye Disease: Diagnosis, Medical Management, Recent Developments, and Future Challenges. Advances in Pharmaceutics. 2015;2015: 1-12.

23. Kinoshita S, Awamura S, Nakamichi N, Suzuki H, Oshiden K, Yokoi N. A Multicenter, Open-Label, 52-Week Study of 2% Rebamipide (OPC-12759) Ophthalmic Suspension in Patients With Dry Eye. Am J Ophthalmol. 2014;1573: 576-83.e1.

24. Senba K, Miyamoto T, Eguchi H, Mitamura Y. The Efficacy Of Oral Pilocarpine For The Treatment Of Dry Eye Symptoms In Patients With Aqueous Tear Deficiency And Evaporative Dry Eye. Invest Ophthalmol Vis Sci. 2011;5214: 3837-.

25. Ono M, Takamura E, Shinozaki K, Tsumura T, Hamano T, Yagi Y, et al. Therapeutic effect of cevimeline on dry eye in patients with Sjögren's syndrome: a randomized, double-blind clinical study. Am J Ophthalmol. 2004;1381: 6-17.

26. Yang C-q, Sun W, Gu Y-s. A clinical study of the efficacy of topical corticosteroids on dry eye. Journal of Zhejiang University Science B. 2006;78: 675-8.

27. Gao J, Sana R, Calder V, Calonge M, Lee W, Wheeler L, et al. Mitochondrial Permeability Transition Pore in Inflammatory Apoptosis of Human Conjunctival Epithelial Cells and T Cells: Effect of Cyclosporin A. Invest Ophthalmol Vis Sci. 2013;54.

28. Moscovici BK, Holzchuh R, Chiacchio BB, Santo RM, Shimazaki J, Hida RY. Clinical Treatment of Dry Eye Using 0.03% Tacrolimus Eye Drops. Cornea. 2012;318.

29. Sawazaki R, Ishihara T, Usui S, Hayashi E, Tahara K, Hoshino T, et al. Diclofenac Protects Cultured Human Corneal Epithelial Cells Against Hyperosmolarity

and Ameliorates Corneal Surface Damage in a Rat Model of Dry Eye. Invest Ophthalmol Vis Sci. 2014;554: 2547-56.

30. Sandoval HP, Fernández de Castro LE, Vroman DT, Solomon KD. A review of the use of ketorolac tromethamine 0.4% in the treatment of post-surgical inflammation following cataract and refractive surgery. Clin Ophthalmol. 2007;14: 367-71.

31. Weber M, Kodjikian L, Kruse F, Zagorski Z, Allaire C. Efficacy and safety of indomethacin 0.1% eye drops compared with ketorolac 0.5% eye drops in the management of ocular inflammation after cataract surgery. Acta Ophthalmol (Copenh). 2012;91.

32. Schmidt TA, Sullivan DA, Knop E, Richards SM, Knop N, Liu S, et al. Transcription, translation, and function of lubricin, a boundary lubricant, at the ocular surface. JAMA ophthalmology. 2013;1316: 766-76.

33. Amparo F, Dastjerdi MH, Okanobo A, Ferrari G, Smaga L, Hamrah P, et al. Topical interleukin 1 receptor antagonist for treatment of dry eye disease: a randomized clinical trial. JAMA ophthalmology. 2013;1316: 715-23.

34. Choi W, Noh H, Yeo A, Jang H, Ahn HK, Song YJ, et al. The Effect of TNF-α Blocker HL036337 and Its Best Concentration to Inhibit Dry Eye Inflammation. Korean journal of ophthalmology : KJO. 2016;304: 302-8.

35. Murube J, Murube E, ChenZhuo L, Rivas L. Subcutaneous abdominal artificial tears pump-reservoir for severe dry eye. Orbit. 2003;221: 29-40.

36. Sekhar L, Bisht N. Stem Cell Therapy. Apollo Medicine. 2006;33: 271-6.

37. He S, Nakada D, Morrison SJ. Mechanisms of Stem Cell Self-Renewal. Annu Rev Cell Dev Biol. 2009;251: 377-406.

38. Takahashi K, Yamanaka S. Induction of pluripotent stem cells from mouse embryonic and adult fibroblast cultures by defined factors. Cell. 2006;1264: 663-76.

39. Karagiannis P, Takahashi K, Saito M, Yoshida Y, Okita K, Watanabe A, et al. Induced Pluripotent Stem Cells and Their Use in Human Models of Disease and Development. Physiol Rev. 2018;991: 79-114.

40. Ronaldson-Bouchard K, Ma SP, Yeager K, Chen T, Song L, Sirabella D, et al. Advanced maturation of human cardiac tissue grown from pluripotent stem cells. Nature. 2018;5567700: 239-43.

41. Lungova V, Chen X, Wang Z, Kendziorski C, Thibeault SL. Human induced pluripotent stem cell-derived vocal fold mucosa mimics development and responses to smoke exposure. Nature Communications. 2019;101: 4161.

42. Low JH, Li P, Chew EGY, Zhou B, Suzuki K, Zhang T, et al. Generation of Human PSC-Derived Kidney Organoids with Patterned Nephron Segments and a De Novo Vascular Network. Cell Stem Cell. 2019;253: 373-87.e9.

43. Akbari S, Sevinç GG, Ersoy N, Basak O, Kaplan K, Sevinç K, et al. Robust, Long-Term Culture of Endoderm-Derived Hepatic Organoids for Disease Modeling. Stem Cell Reports. 2019;134: 627-41.

44. Mandai M, Watanabe A, Kurimoto Y, Hirami Y, Morinaga C, Daimon T, et al. Autologous Induced Stem-Cell–Derived Retinal Cells for Macular Degeneration. N Engl J Med. 2017;37611: 1038-46.

45. Khademhosseini A, Langer R. A decade of progress in tissue engineering. Nat Protoc. 2016;1110: 1775-81.

46. Berthiaume F, Maguire TJ, Yarmush ML. Tissue Engineering and Regenerative Medicine: History, Progress, and Challenges. Annual Review of Chemical and Biomolecular Engineering. 2011;21: 403-30.

47. Ueda Y, Karasawa Y, Satoh Y, Nishikawa S, Imaki J, Ito M. Purification and characterization of mouse lacrimal gland epithelial cells and reconstruction of an

acinarlike structure in three-dimensional culture. Invest Ophthalmol Vis Sci. 2009;505: 1978-87.

48. Tiwari S, Ali MJ, Balla MM, Naik MN, Honavar SG, Reddy VA, et al. Establishing human lacrimal gland cultures with secretory function. PLoS One. 2012;71: e29458.

49. Lin H, Sun G, He H, Botsford B, Li M, Elisseeff JH, et al. Three-Dimensional Culture of Functional Adult Rabbit Lacrimal Gland Epithelial Cells on Decellularized Scaffold. Tissue Engineering Part A. 2015;221-2: 65-74.

50. Schrader S, Wedel T, Kremling C, Laqua H, Geerling G. Amniotic membrane as a carrier for lacrimal gland acinar cells. Graefes Arch Clin Exp Ophthalmol. 2007;24511: 1699-704.

51. Hirayama M, Ogawa M, Oshima M, Sekine Y, Ishida K, Yamashita K, et al. Functional lacrimal gland regeneration by transplantation of a bioengineered organ germ. Nat Commun. 2013;4: 2497.

52. Hayashi R, Ishikawa Y, Sasamoto Y, Katori R, Nomura N, Ichikawa T, et al. Co-ordinated ocular development from human iPS cells and recovery of corneal function. Nature. 2016;5317594: 376-80.

53. Hayashi R, Ishikawa Y, Katori R, Sasamoto Y, Taniwaki Y, Takayanagi H, et al. Coordinated generation of multiple ocular-like cell lineages and fabrication of functional corneal epithelial cell sheets from human iPS cells. Nat Protoc. 2017;124: 683-96.

54. Li Z, Duan H, Li W, Hu X, Jia Y, Zhao C, et al. Rapid Differentiation of Multi-Zone Ocular Cells from Human Induced Pluripotent Stem Cells and Generation of Corneal Epithelial and Endothelial Cells. Stem Cells and Development. 2019;287: 454-63.

55. Susaimanickam PJ, Maddileti S, Pulimamidi VK, Boyinpally SR, Naik RR, Naik MN, et al. Generating minicorneal organoids from human induced pluripotent stem cells. Development. 2017;14413: 2338-51.

56. Farmer DJT, Nathan S, Finley JK, Shengyang Yu K, Emmerson E, Byrnes LE, et al. Defining epithelial cell dynamics and lineage relationships in the developing lacrimal gland. Development (Cambridge, England). 2017;14413: 2517-28.

57. Mattiske D, Sommer P, Kidson SH, Hogan BLM. The role of the forkhead transcription factor, Foxc1, in the development of the mouse lacrimal gland. Developmental dynamics : an official publication of the American Association of Anatomists. 2006;2354: 1074-80.

58. Okami T, Yamamoto A, Takada T, Omori K, Uyama M, Tashiro Y. Ultrastructural localization of Na+, K(+)-ATPase in the exorbital lacrimal gland of rat. Invest Ophthalmol Vis Sci. 1992;331: 196-204.

59. Hirayama M, Ko SBH, Kawakita T, Akiyama T, Goparaju SK, Soma A, et al. Identification of transcription factors that promote the differentiation of human pluripotent stem cells into lacrimal gland epithelium-like cells. NPJ Aging Mech Dis. 2017;3: 1.

60. Shibata S, Hayashi R, Okubo T, Kudo Y, Katayama T, Ishikawa Y, et al. Selective Laminin-Directed Differentiation of Human Induced Pluripotent Stem Cells into Distinct Ocular Lineages. Cell Rep. 2018;256: 1668-79 e5.

8. APPENDIX

8.1. Ethics Committee Approval

İZMİR BİYOTIP VE GENOM MERKEZİ
GİRİŞİMSEL OLMAYAN ARAŞTIRMALAR ETİK KURULU (İBG-GOEK)
KARARI

Toplantı Tarihi	: 16/05/2020	**Toplantı Günü**	: Cumartesi
Toplantı Sayısı	: 6	**Toplantı Saati**	: 13:00

Sayın Sinan GÜVEN,

2020-019 Protokol No'lu; sorumlusu olduğunuz "Uyarılmış pluripotent kök hücreler kullanılarak lakrimal bezin geliştirilmesi" başlıklı araştırmanın uygulanmasında etik açıdan sakınca olmadığına oy birliği ile karar verilmiştir.

Bilgilerinizi ve gereğini rica ederiz.

Prof. Dr. H. Alper BAĞRIYANIK
Başkan

Pandemi süresince online ortamda gerçekleştirilen toplantımızda alınan kararlar tek imzalı olarak düzenlenmektedir. Pandemi sona erdikten sonra ıslak imzalı karar belgesi teslim edilecektir.

8.2. Curriculum Vitae

Melis Asal

ID Number:	18107333242
Date of Birth:	06.11.1994
Contact Address:	540 sokak no:1 da:8 Zafertepe Mahallesi Konak/Izmir
Phone :	+90 538 504 5279
e-mail:	melis_asal@hotmail.com

EDUCATIONAL BACKGROUND

Country	University	Faculty/ Institute	Department	Degree	Year of Graduation
Turkey	Manisa Celal Bayar University	Engineering	Bioengineering	Bachelor's	2017
Turkey	Dokuz Eylul University	Izmir Biomedicine and Genome Institute	Molecular Biology and Genetics	Master of Science	2020

ACADEMIC / PROFESSIONAL EXPERIENCE

Institution	Country	City	Department	Position	Year
GENMAR Teşhis Ürünleri Ar-Ge Laboratuvar Hizmetleri San. Tic. Ltd.	Turkey	Izmir	Molecular Biology and Genetics	Internship	July 2015
Pınar Entegre Et ve Un San. A.Ş.	Turkey	Izmir	Microbiology and Quality Assurance	Internship	July 2016
Institut Pasteur	France	Paris	Bacterial Genome Plasticity	Internship	July-August 2017

Institut Pasteur	France	Paris	Physical Microfluidics and Bioengineering	Internship	July-August 2018

SPECIALIZED FIELDS

Lacrimal Gland, Induced Pluripotent Stem Cells, Tissue Engineering, Regenerative Medicine

AWARDS

Name of the Reward	Organization	Year
3rd Place in the Engineering Category	Manisa Celal Bayar University 24th Science and Spring Festival Science Projects Contest	2017
Poster Award, 3rd Place	Biomedical Science and Technology Symposium	2018

ARTICLES PUBLISHED IN SCI, SSCI, AHCI INDEXED JOURNALS

Asal, M., Özen, Ö., Şahinler, M., Polatoğlu, İ. (2018). Recent Developments in Enzyme, DNA and Immuno-Based Biosensors. *Sensors (Basel),* 18(6).
Asal, M., Özen, Ö., Şahinler, M., Baysal, H. and Polatoğlu, İ. (2018). An Overview of Biomolecules, Immobilization Methods and Support Materials of Biosensors. *Sensor Review*, 39(3), pp. 377-386.

ABSTRACTS PUBLISHED IN CONFERENCE PROCEEDINGS

INTERNATIONAL CONFERENCES
Sönmez Kılıçarslan P., Toros P., **Asal M.**, Şahinler M., Tuğlu., İ. M. 'Deneysel Yara Oluşturulmuş Sıçanlarda Kök Hücre ve Kekik Yağının Yara İyileşmesi Üzerine Etkisi' 2nd International Graduate Education Congress, Manisa, 12-14 May 2017
Asal, M., Yıldırım, C.A., Güven, S. 'Induced Pluripotent Stem Cells (iPSC) Derived Lacrimal Gland' 24th International Biomedical Science and Technology Symposium, İzmir, 17-20 October 2019
Baş, A.K., **Asal, M.**, Kasal., K., Akbulud, O.B., Yıldırım, C.A., Güven, S. ' Bioengineering of Lacrimal Gland in Microfludics' 24th International Biomedical

Science and Technology Symposium, İzmir, 17-20 October 2019
Asal, M., Yıldırım, C.A., Güven, S. 'Lacrimal Gland on Chip Derived from Induced Pluripotent Stem Cells' EMBL IBEC Winter Conference on Engineering Multicellular Systems, Barcelona, 10-12 February 2020
Utine, A.C., **Asal, M.**, Güven, S. 'Induced Pluripotent Stem Cells Derived Lacrimal Gland' ARVO Annual Meeting, 2020
NATIONAL CONFERENCES
Özen Ö., Baysal H.T., **Asal M.**, Şahinler M. '*In vitro* Ortamda L929 Hücre Hattında Oluşturulan Yara Modelinde Kök Hücre ve Kekik Yağının İyileşme Sürecine Etkileri' 2nd Life Sciences Congress, Kayseri, 23-25 February 2017
Baş, A.K., **Asal, M.**, Kasal., K., Akbulud, O.B., Yanık, H., Yıldırım, C.A., Güven, S. 'Doku Mühendisliği Yöntemiyle Kök Hücreler Kullanarak Lakrimal Bezin Geliştirilmesi' 5th Biomaterial Days, İstanbul, 22-23 October 2018
Baş, A.K., **Asal, M.**, Kasal., K., Akbulud, O.B., Yanık, H., Yıldırım, C.A., Güven, S. 'Lakrimal Doku Mühendisliği' 23rd Biomedical Science and Technology Symposium, İstanbul, 15-16 December 2018

BOOKS

Erbay, İ., Baş, A., **Asal, M.**, Yanık, H., Güven, S. (2018). Mikroakışkan Sistemler ve Doku Mühendisliği. İleri Malzemeler: Biyomalzeme ve Nanomalzeme Uygulamaları. Palme Yayınları.
Asal, M., & Güven, S. (2020). Stem Cells: Sources, Properties, and Cell Types. In Biomaterials for Organ and Tissue Regeneration (pp. 177–196). Elsevier.